PNN' & P_2NN' Ligands via Reductive Amination with Phosphine Aldehydes: Synthesis and Base-Metal Coordination Chemistry

Matthew V. Gradiski, Brian T. H. Tsui, Alan J. Lough and Robert H. Morris*

Davenport Chemical Research Laboratories, Department of Chemistry, University of Toronto

80 St. George Street

, Toronto, Ontario, Canada, M5S 3H6

1. NMR spectra……S2

2. X-ray structure of 1a……S47

3. Crystal data and structure refinements of 1a, 4-11…….S48

4. Solid State Magnetic Data of 9 and 10…….S57

5. Base-Study of STAB and Phenyl-Phosphonium Dimer……S60

6. References……..S63

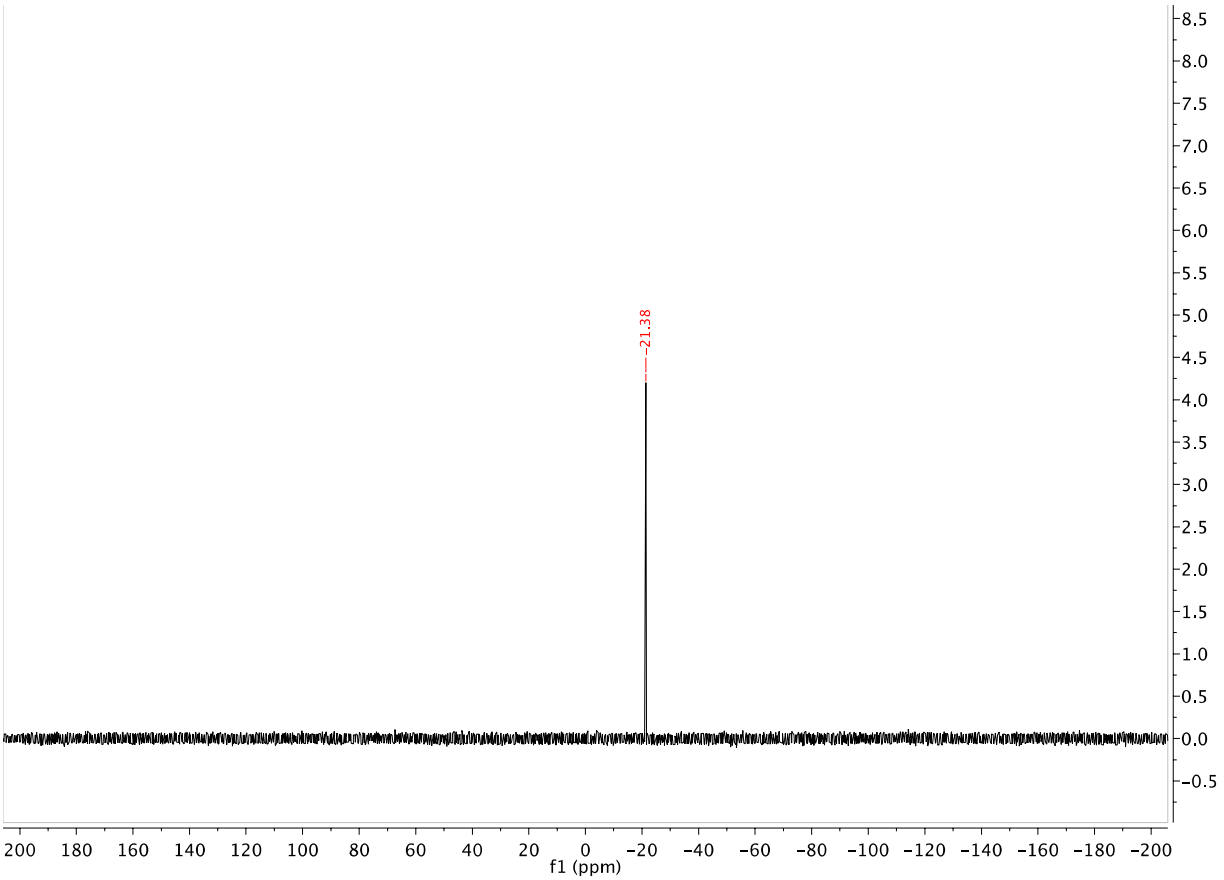

Figure S1. $^{31}P\{^{1}H\}$ NMR spectrum (202 MHz, $CDCl_3$) of APyPNN-Ph **1a**

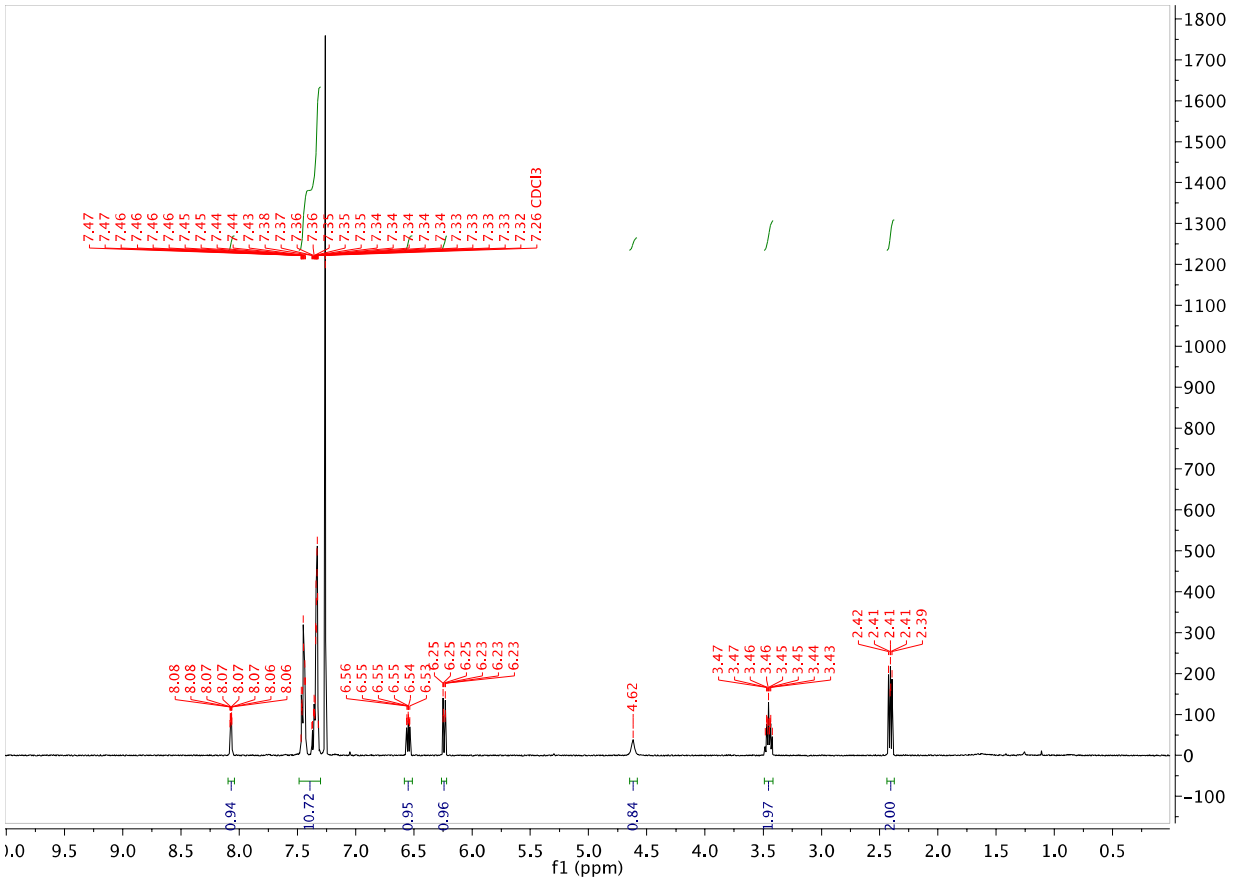

Figure S2. ^{1}H NMR spectrum (500 MHz, $CDCl_3$) of APyPNN-Ph **1a**

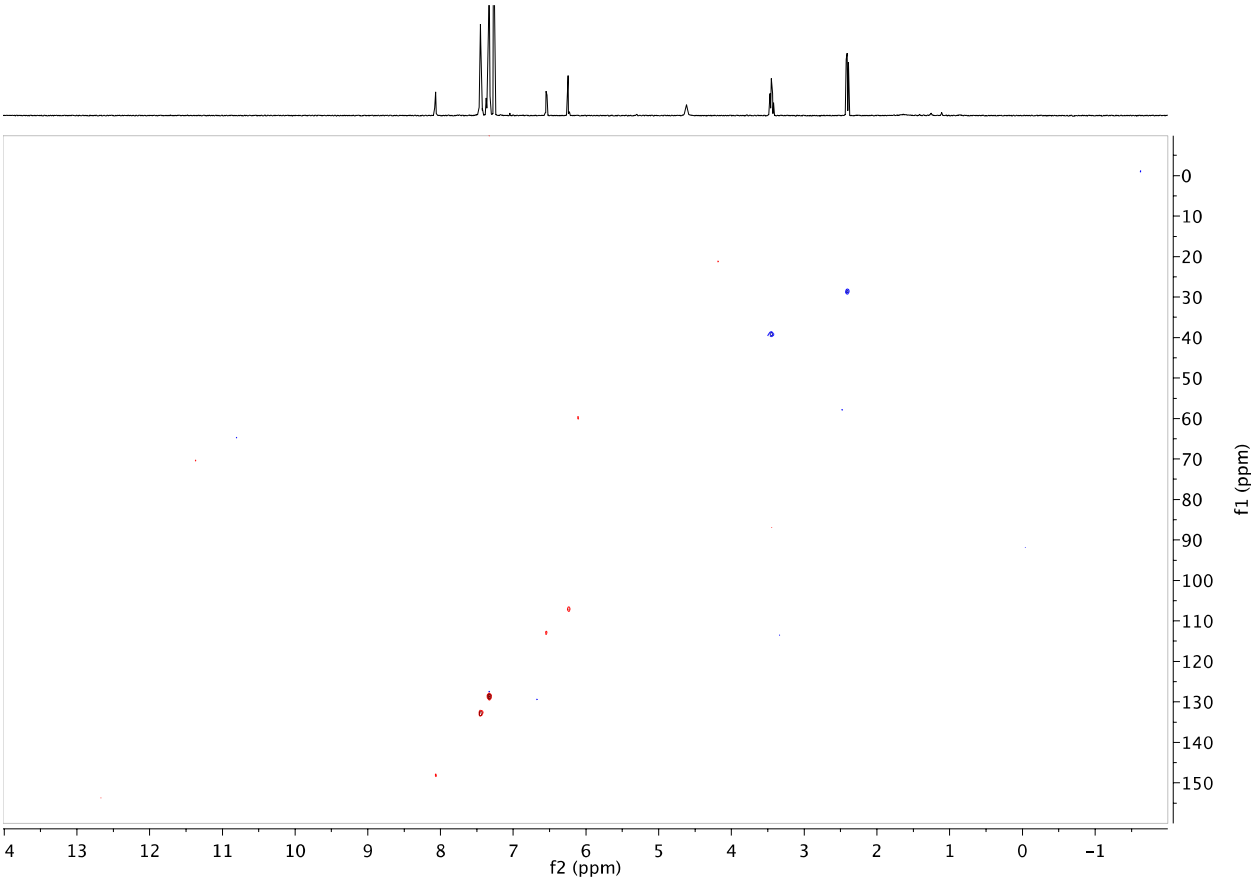

Figure S3. $^{1}H–^{13}C$ gHSQC spectrum of APyPNN-Ph **1a**

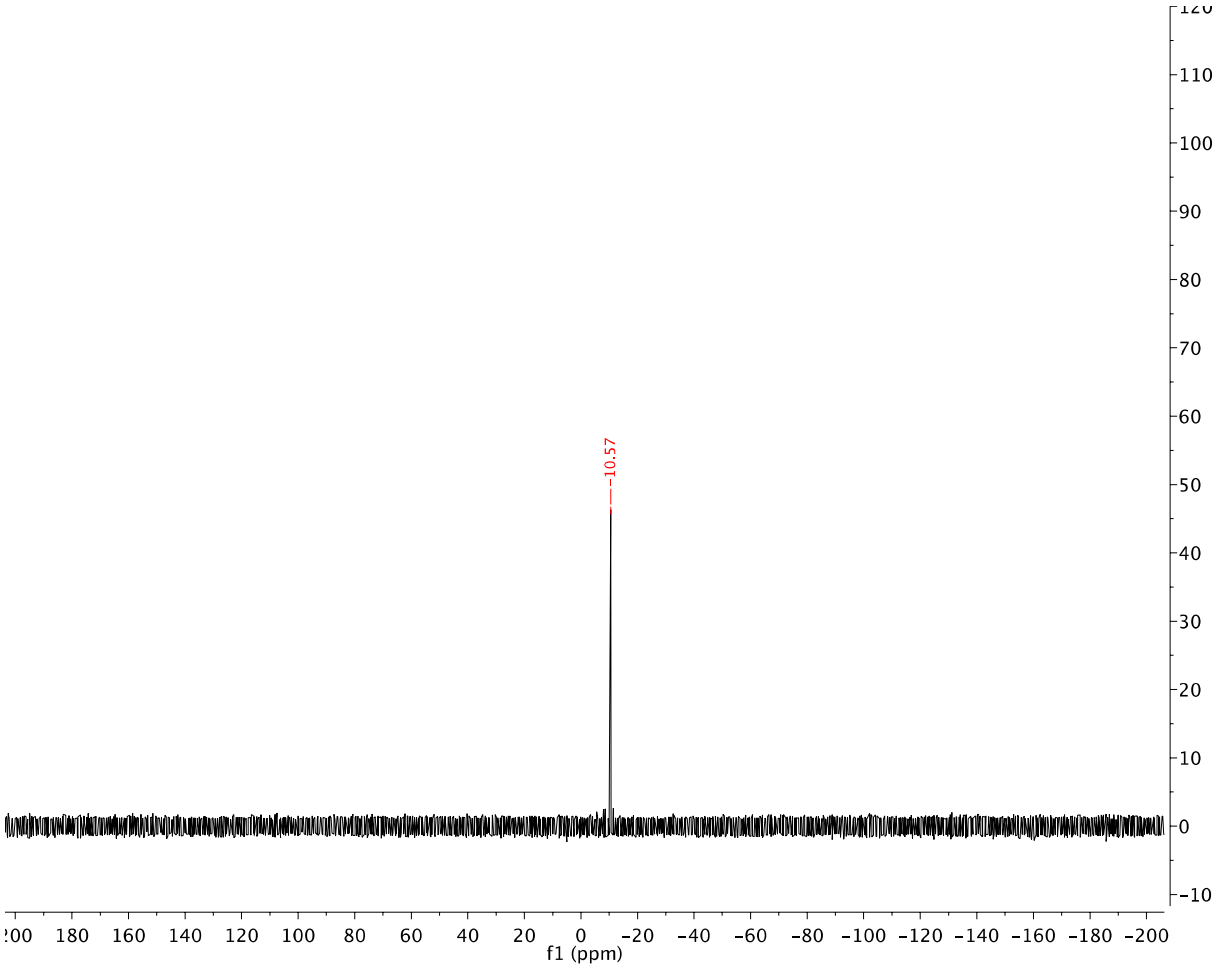

Figure S4. $^{31}P\{^{1}H\}$ NMR spectrum (242 MHz, $CDCl_3$) of APyPNN-Cy **1b**

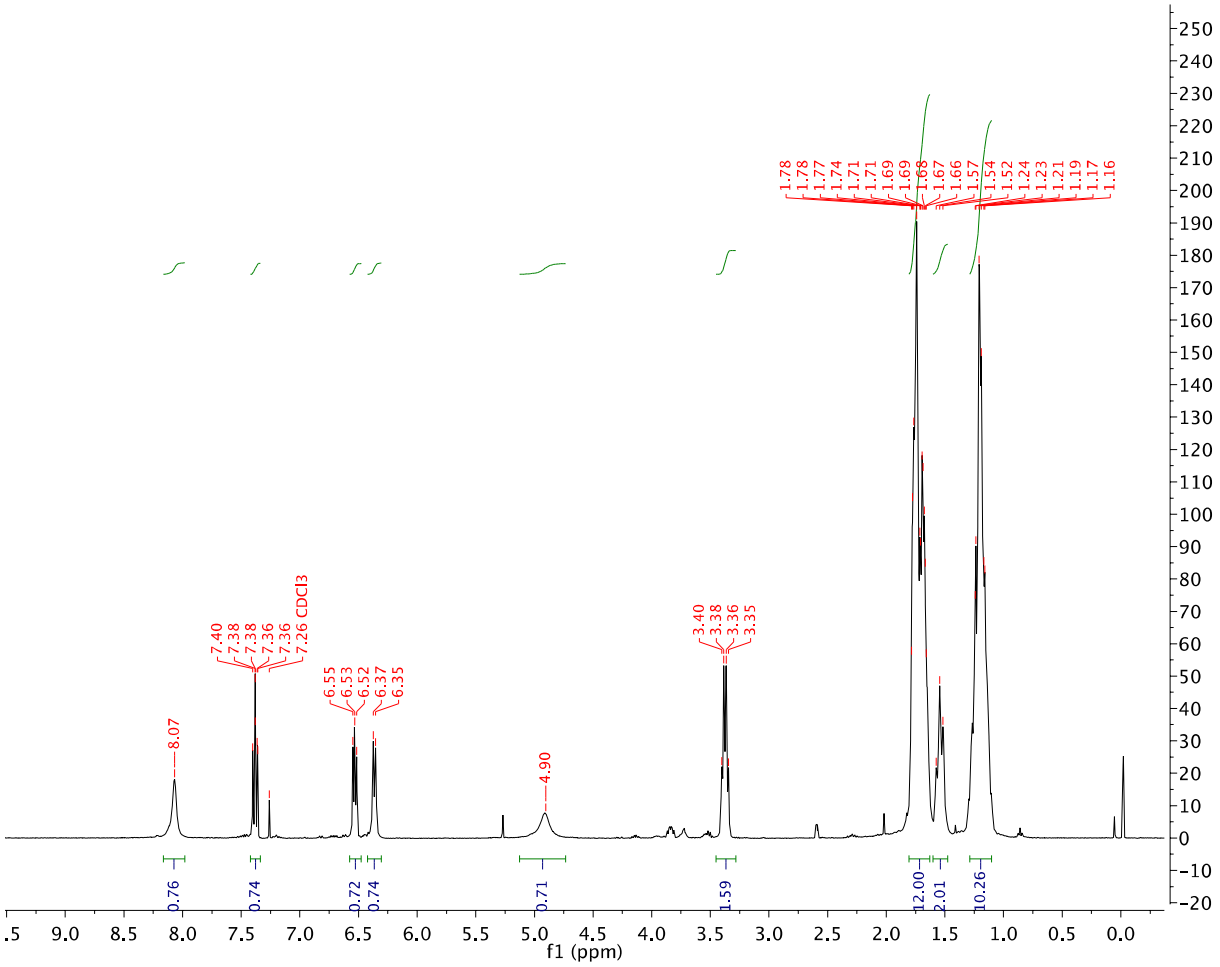

Figure S5. ^{1}H NMR spectrum (500 MHz, $CDCl_3$) of APyPNN-Cy **1b**

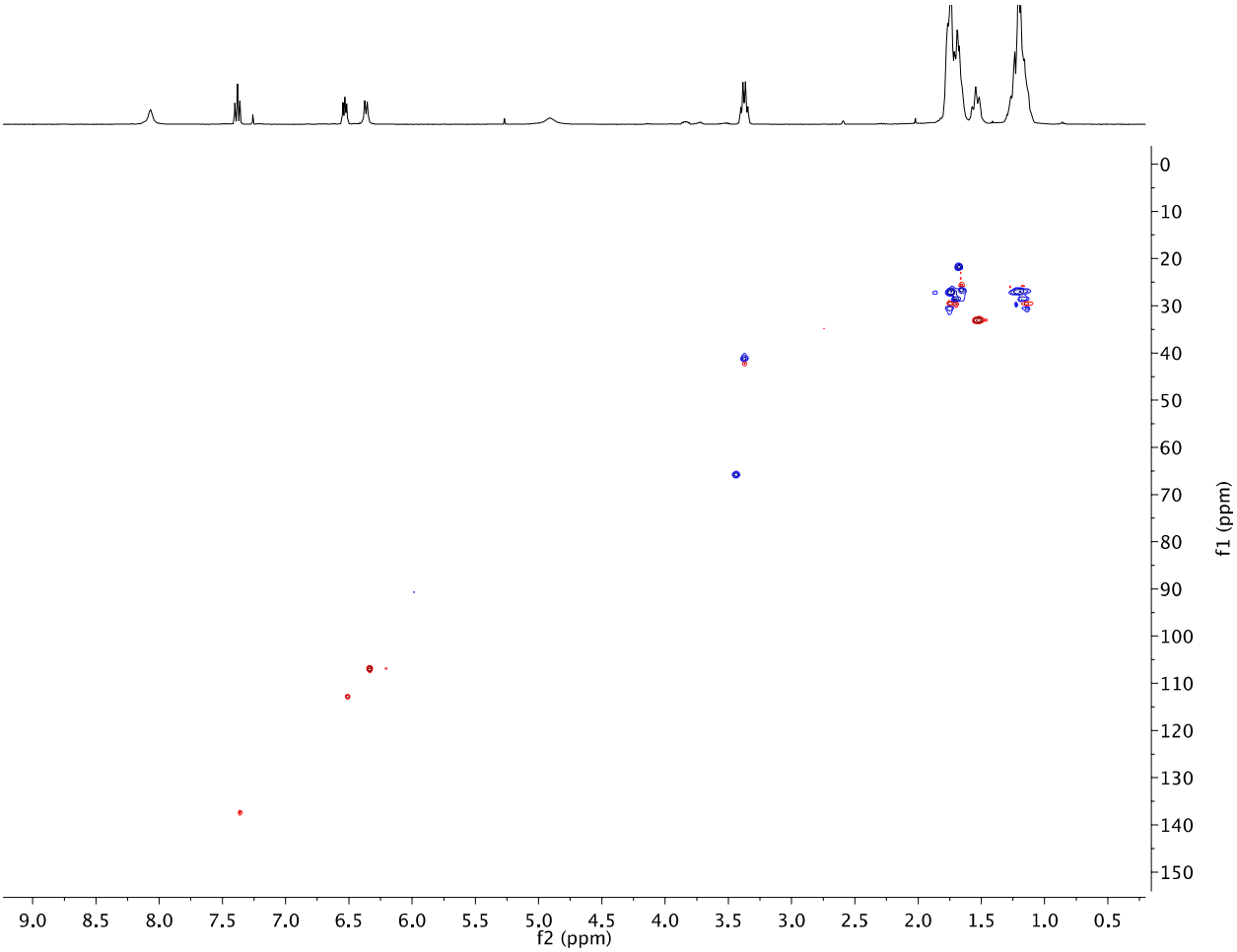

Figure S6. $^{1}H–^{13}C$ gHSQC spectrum of APyPNN-Cy **1b**

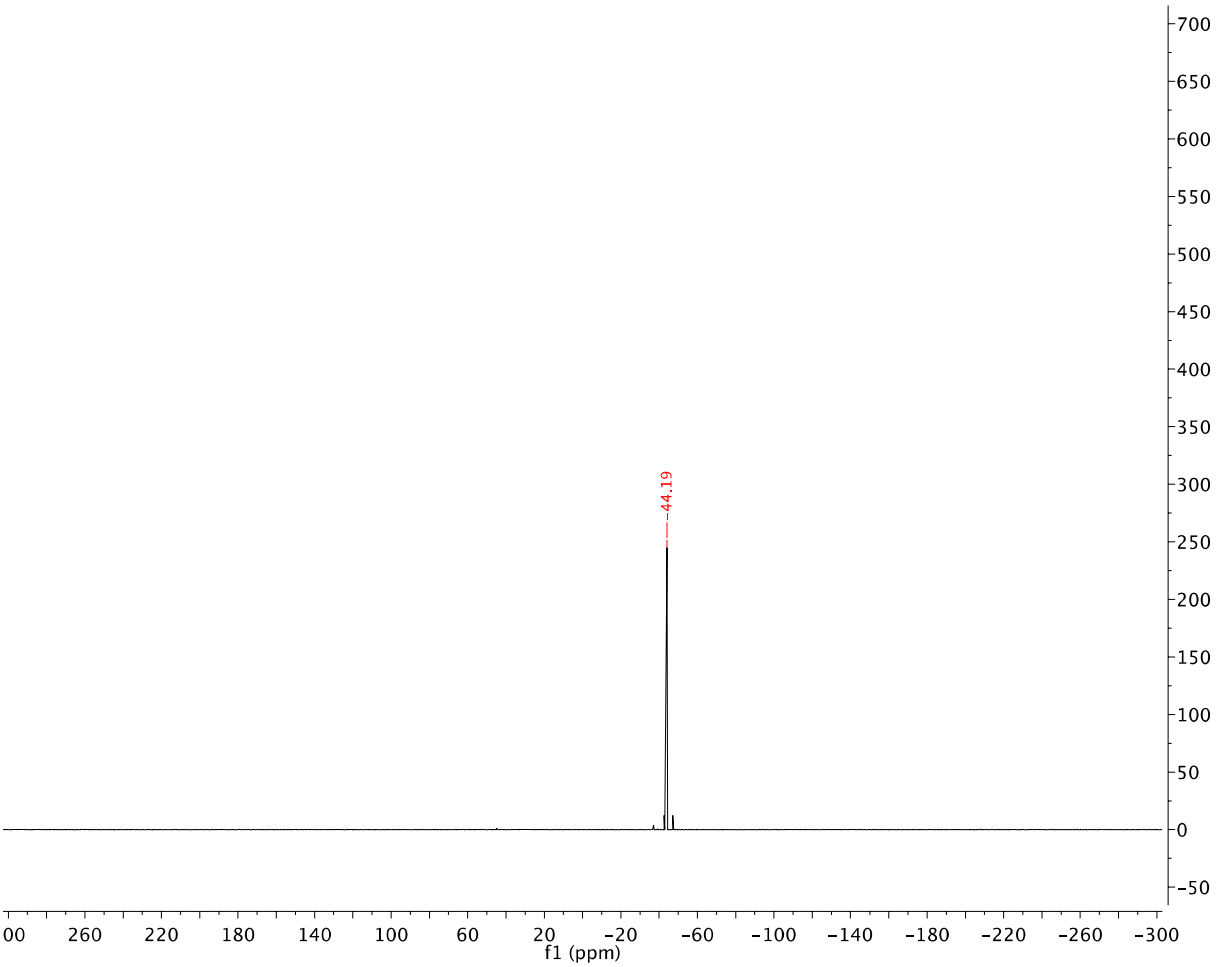

Figure S7. $^{31}P\{^{1}H\}$ NMR spectrum (202 MHz, $CDCl_3$) of APyPNN-^{i}Bu **1c**

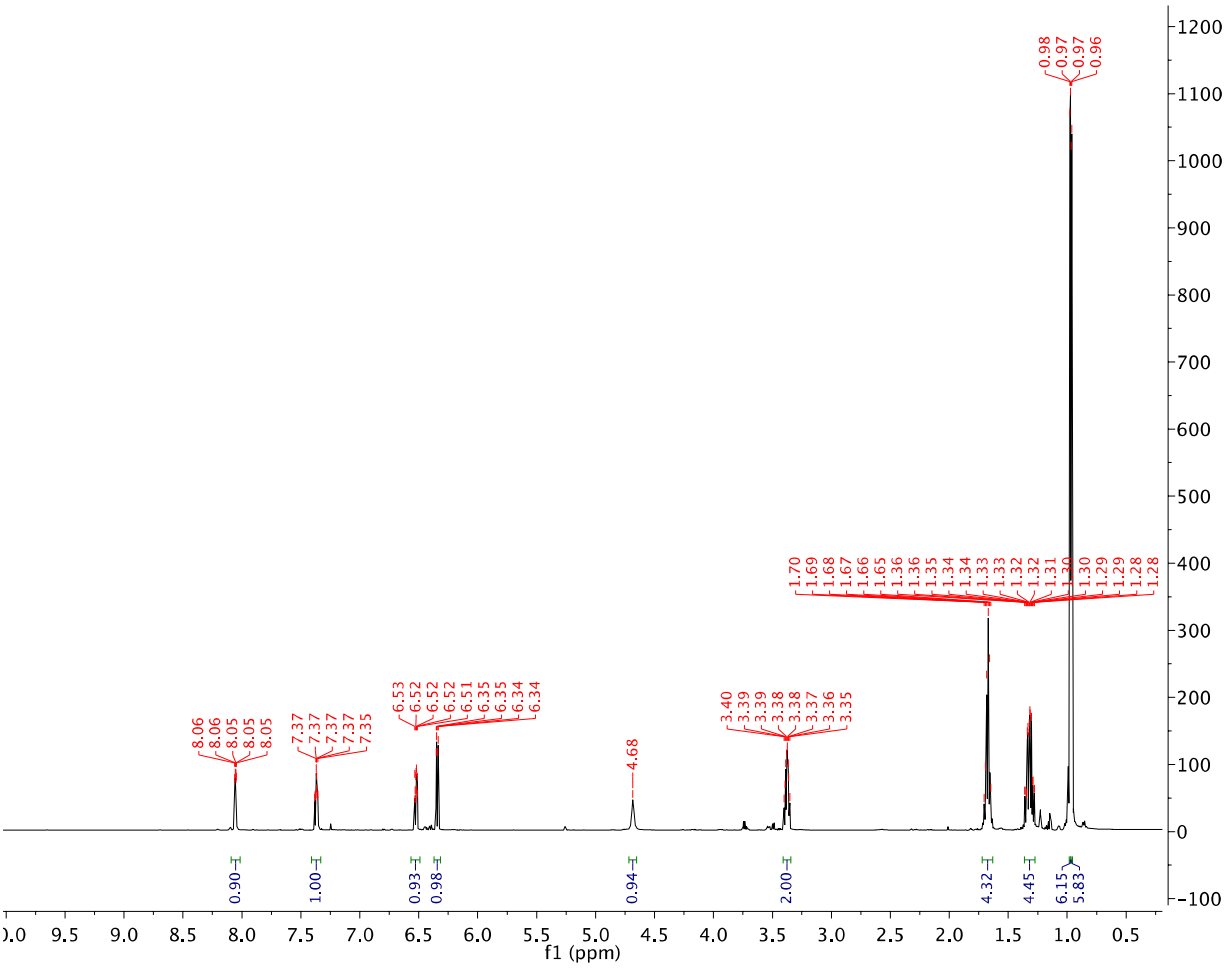

Figure S8. ^{1}H NMR spectrum (500 MHz, $CDCl_3$) of APyPNN-^{i}Bu **1c**

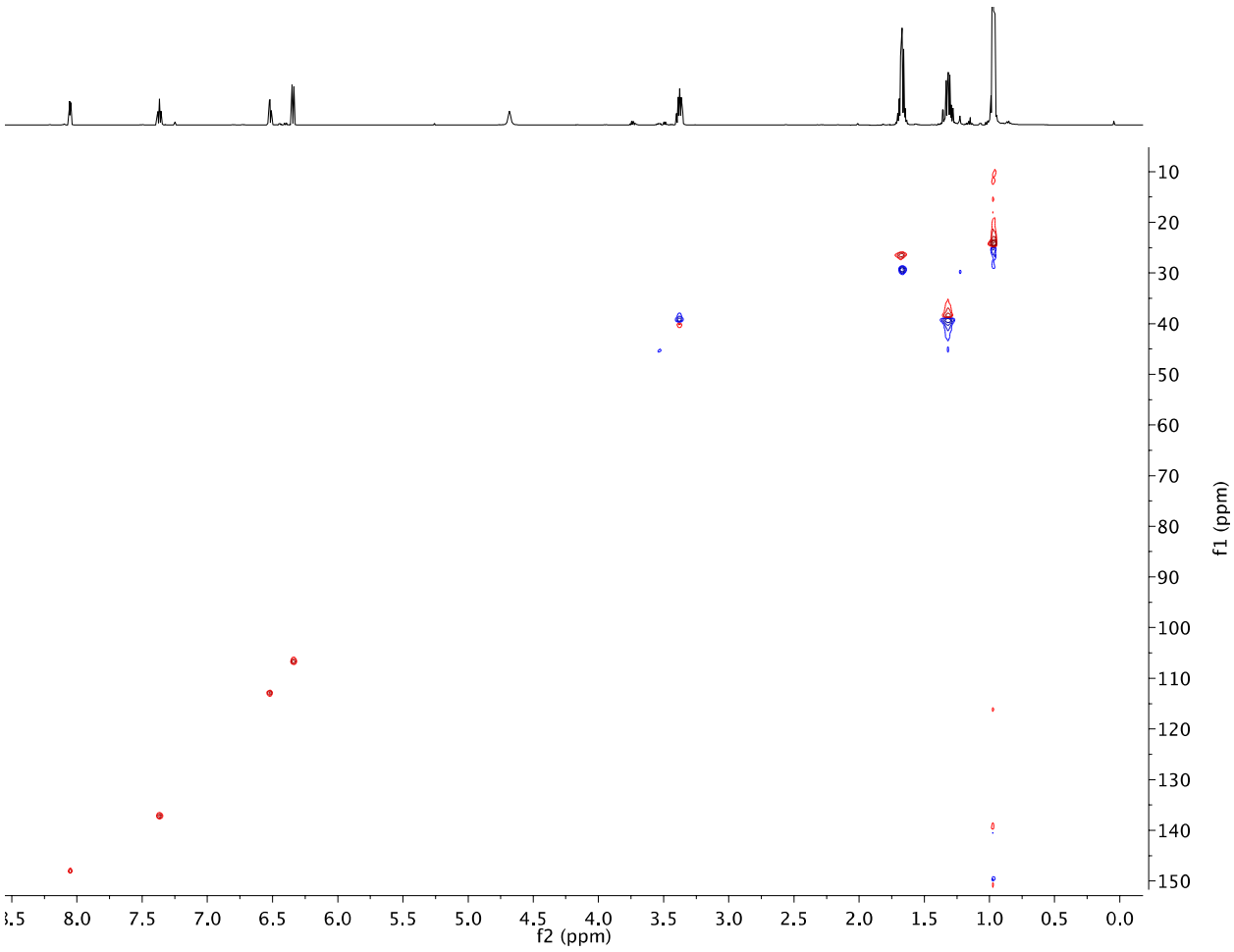

Figure S9. $^{1}H–^{13}C$ gHSQC spectrum of APyPNN-^{i}Bu **1c**

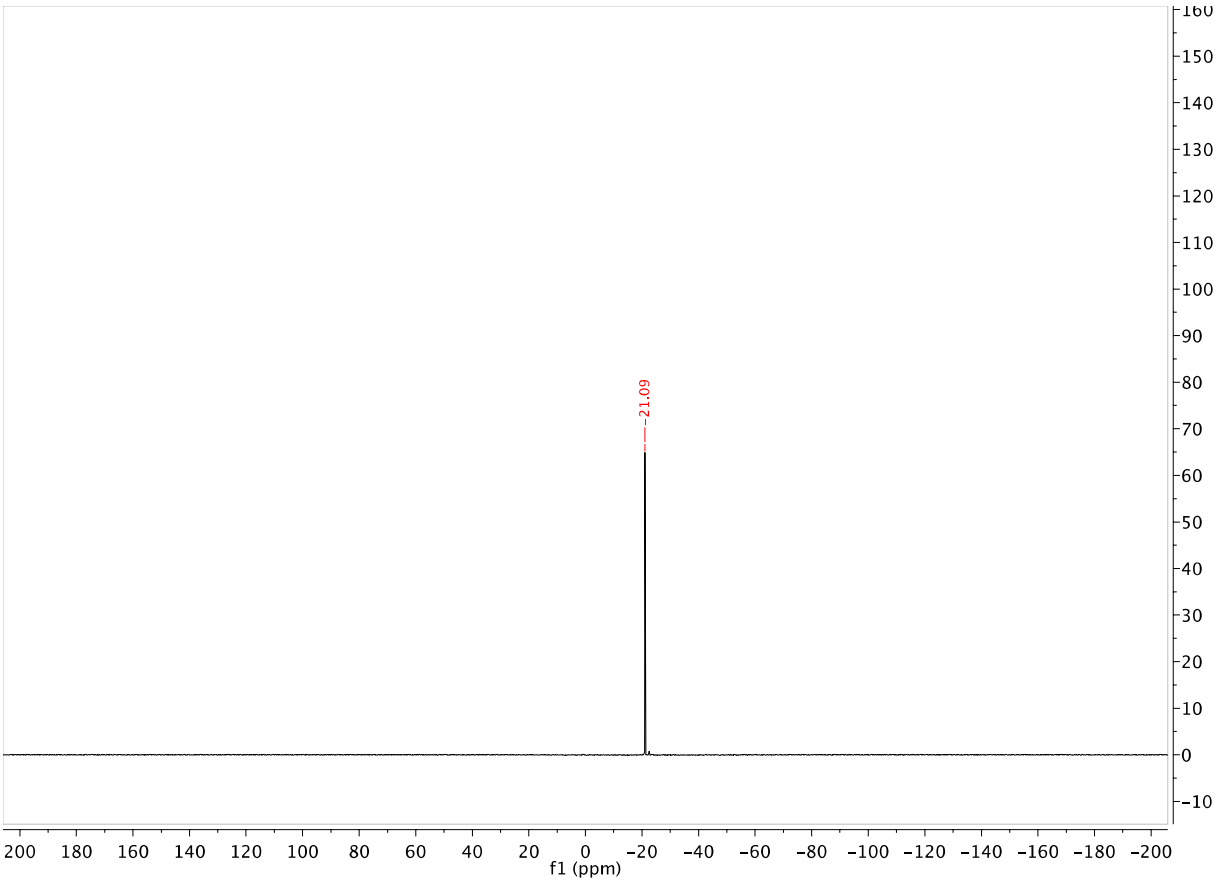

Figure S10. $^{31}P\{^{1}H\}$ NMR spectrum (202 MHz, $CDCl_3$) of AQPNN-Ph **2a**

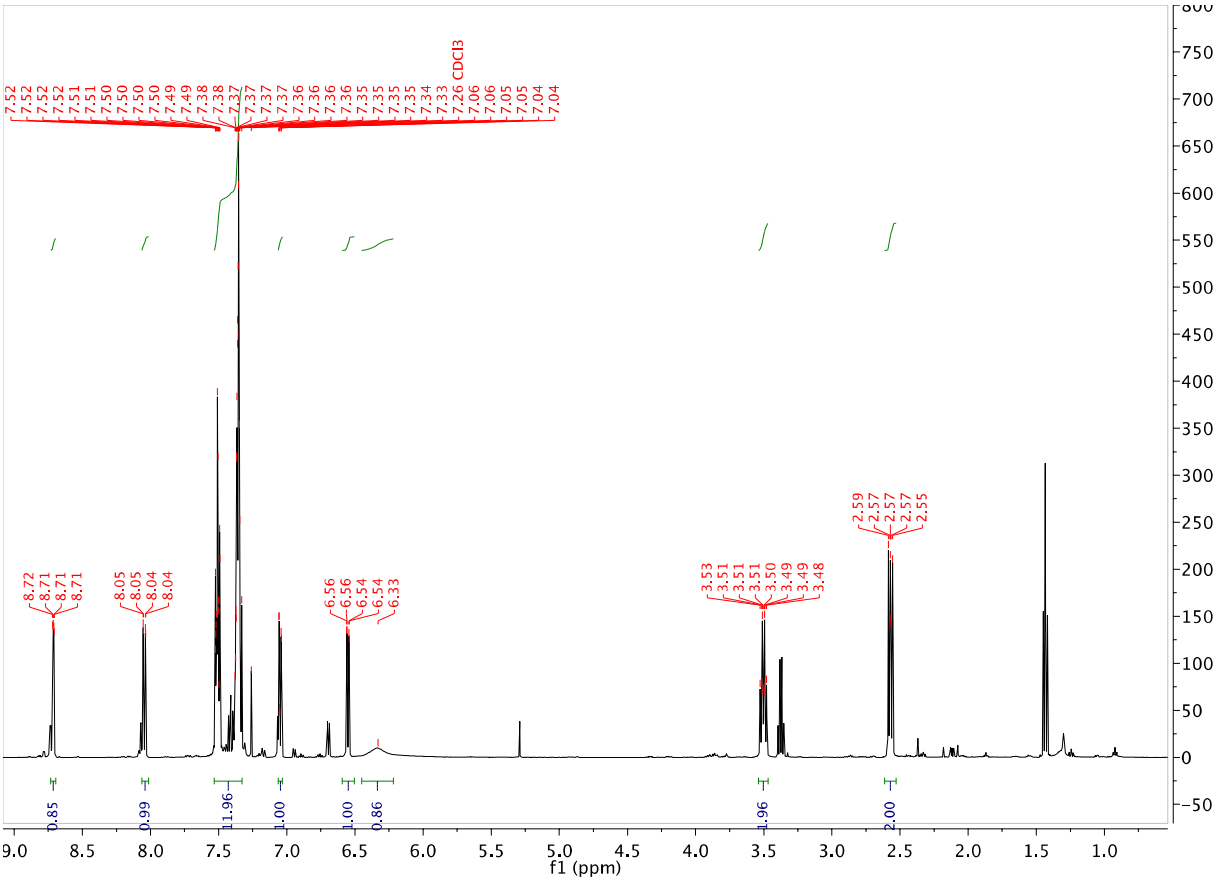

Figure S11. ^{1}H NMR spectrum (500 MHz, $CDCl_3$) of AQPNN-Ph **2a**

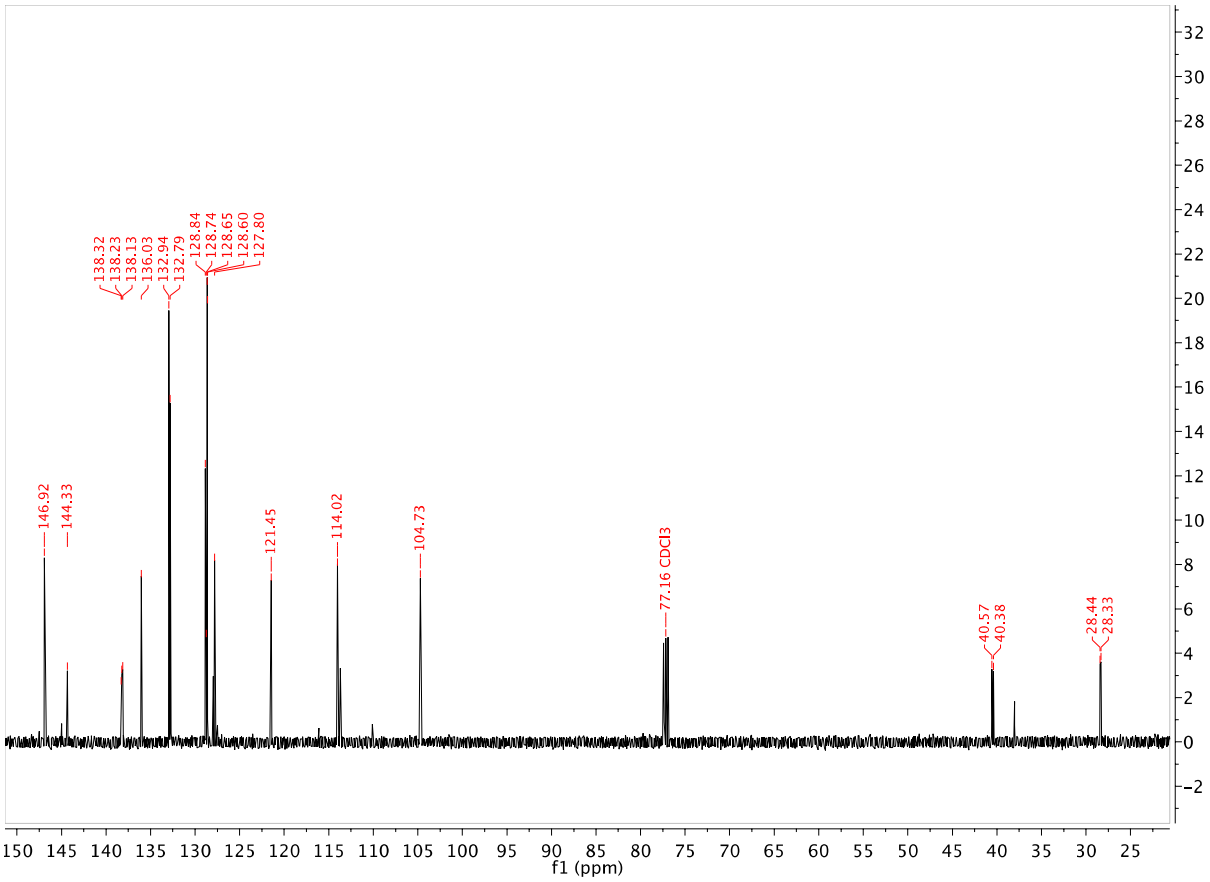

Figure S12. ^{13}C NMR spectrum (126 MHz, $CDCl_3$) of AQPNN-Ph **2a**

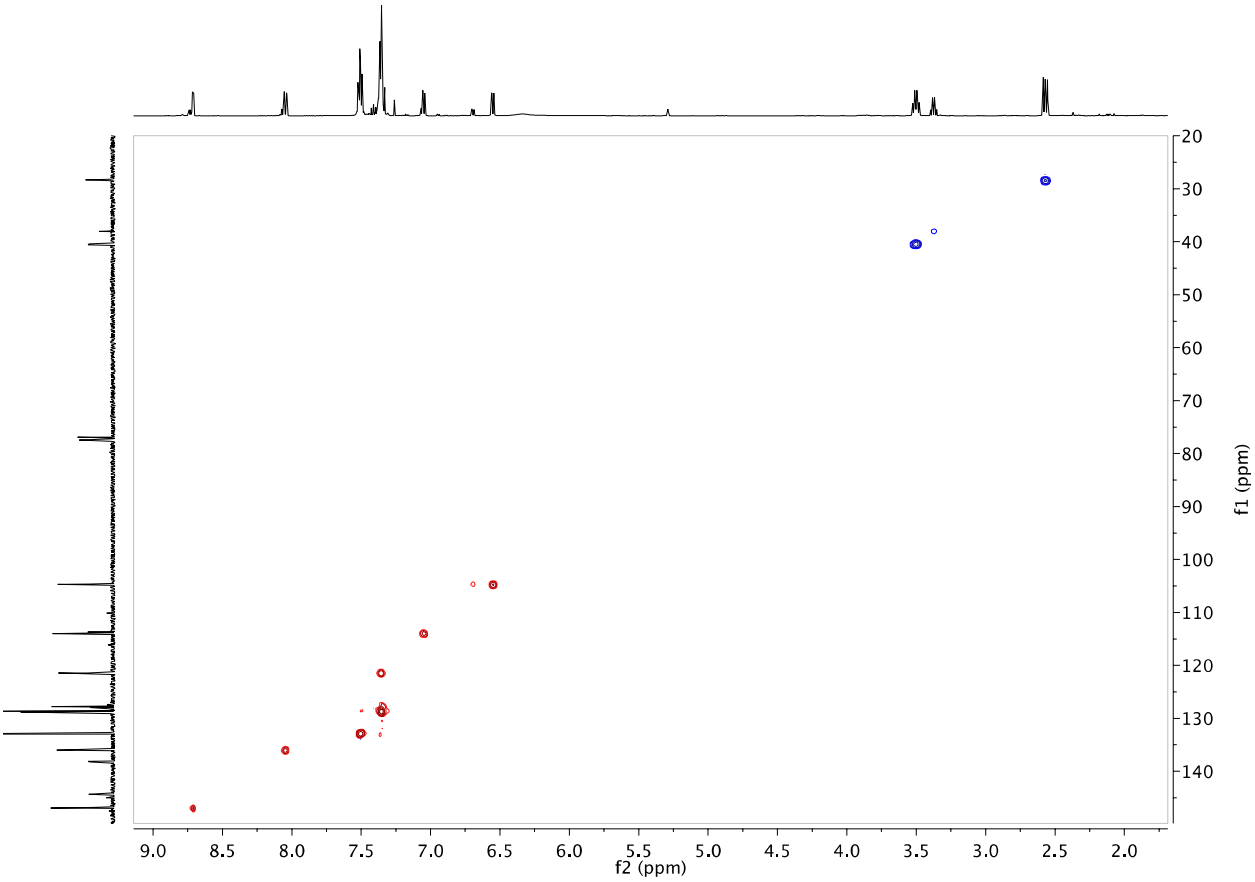

Figure S13. ^{1}H–^{13}C gHSQC spectrum of AQPNN-Ph **2a**

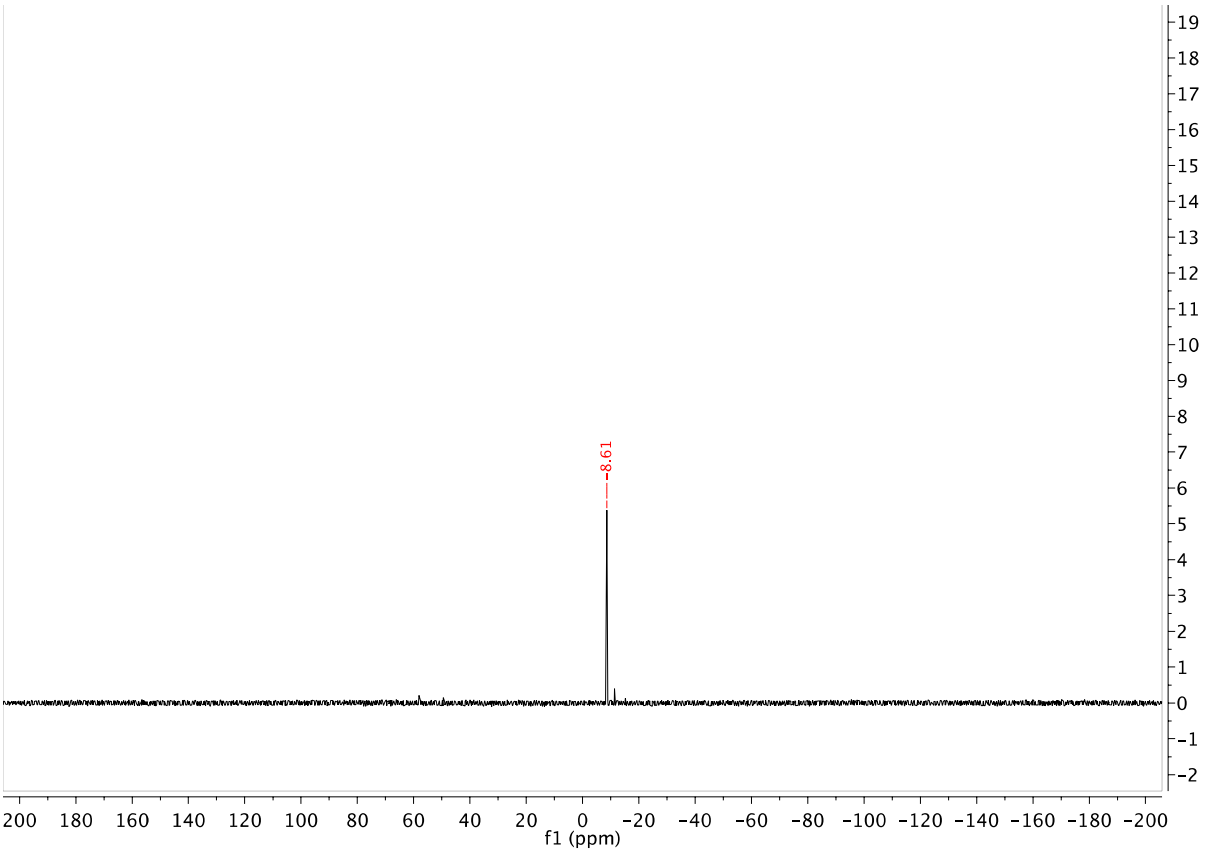

Figure S14. $^{31}P\{^{1}H\}$ NMR spectrum (202 MHz, $CDCl_3$) of AQPNN-Cy **2b**

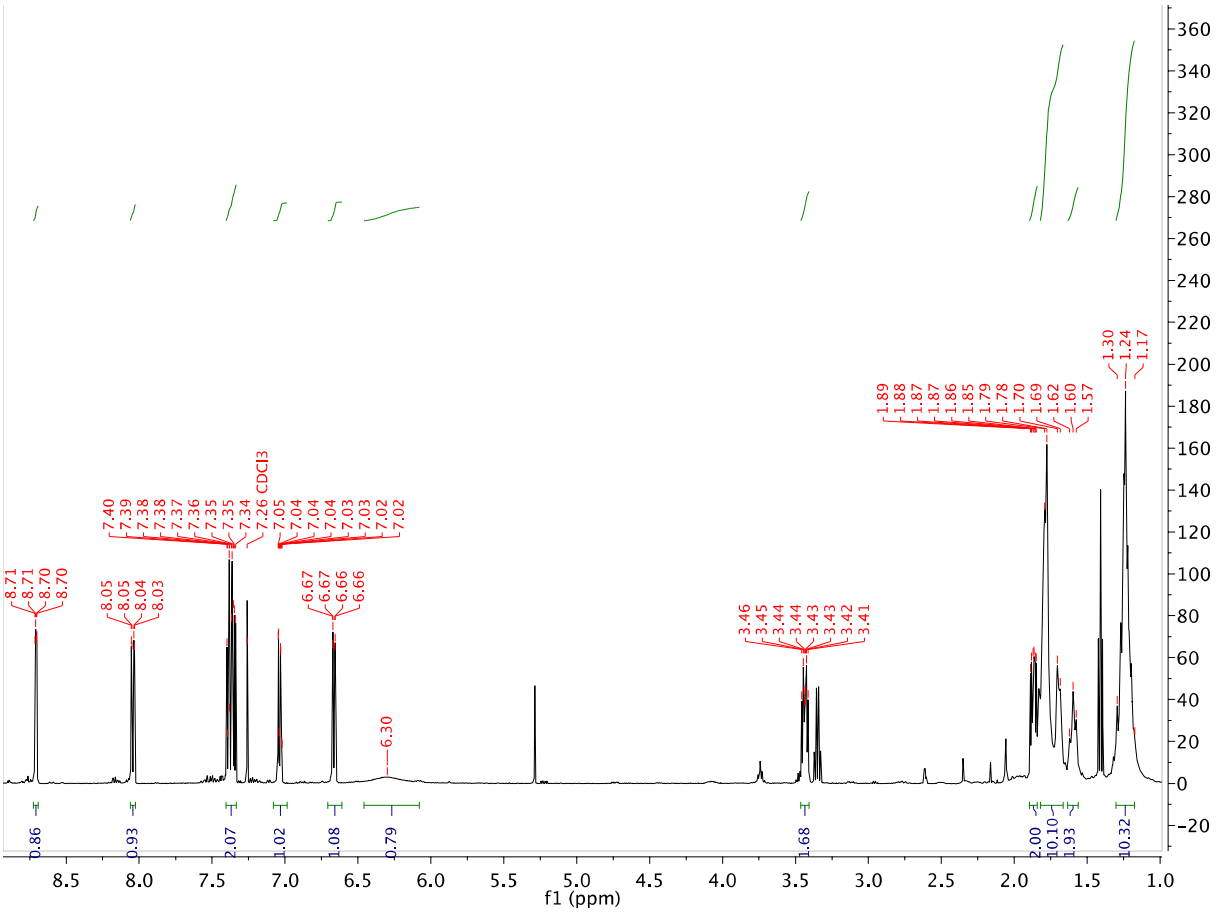

Figure S15. ^{1}H NMR spectrum (500 MHz, $CDCl_3$) of AQPNN-Cy **2b**

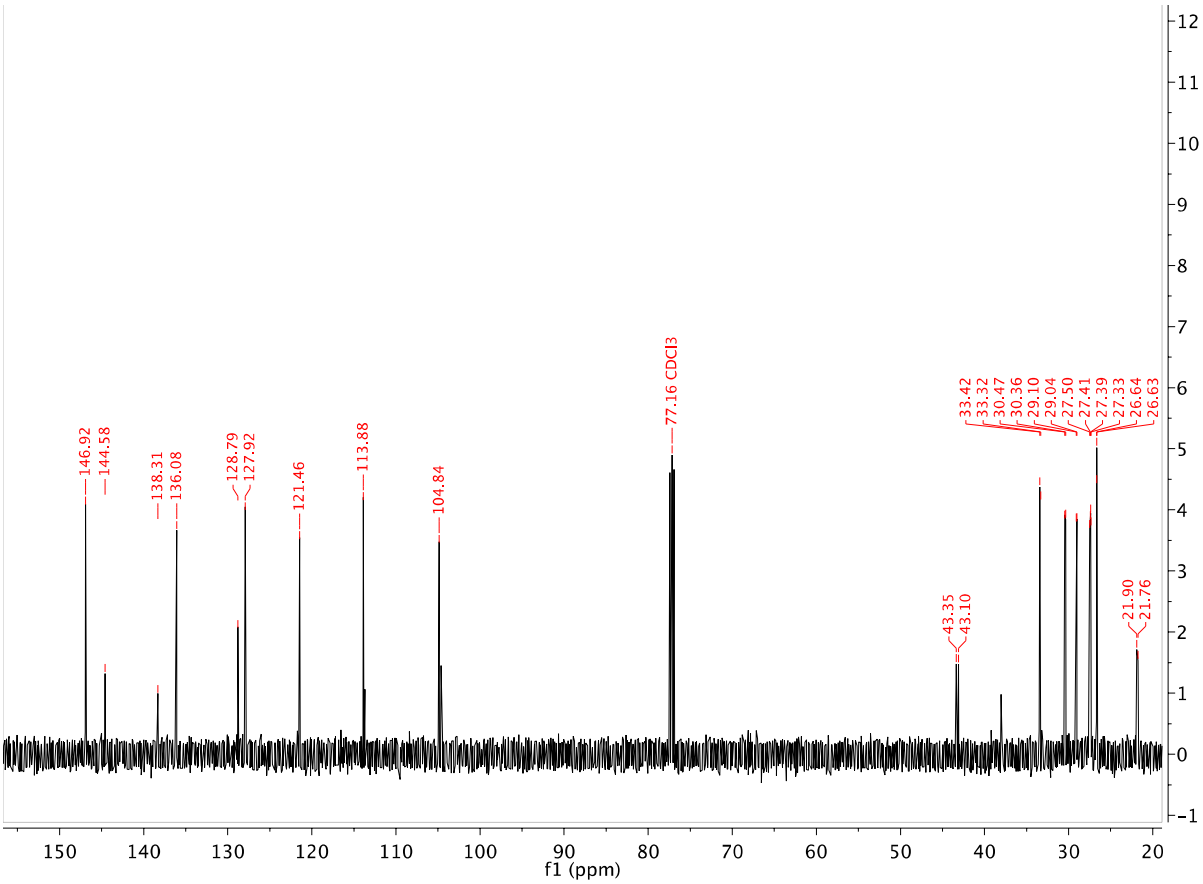

Figure S16. ^{13}C NMR spectrum (126 MHz, $CDCl_3$) of AQPNN-Cy **2b**

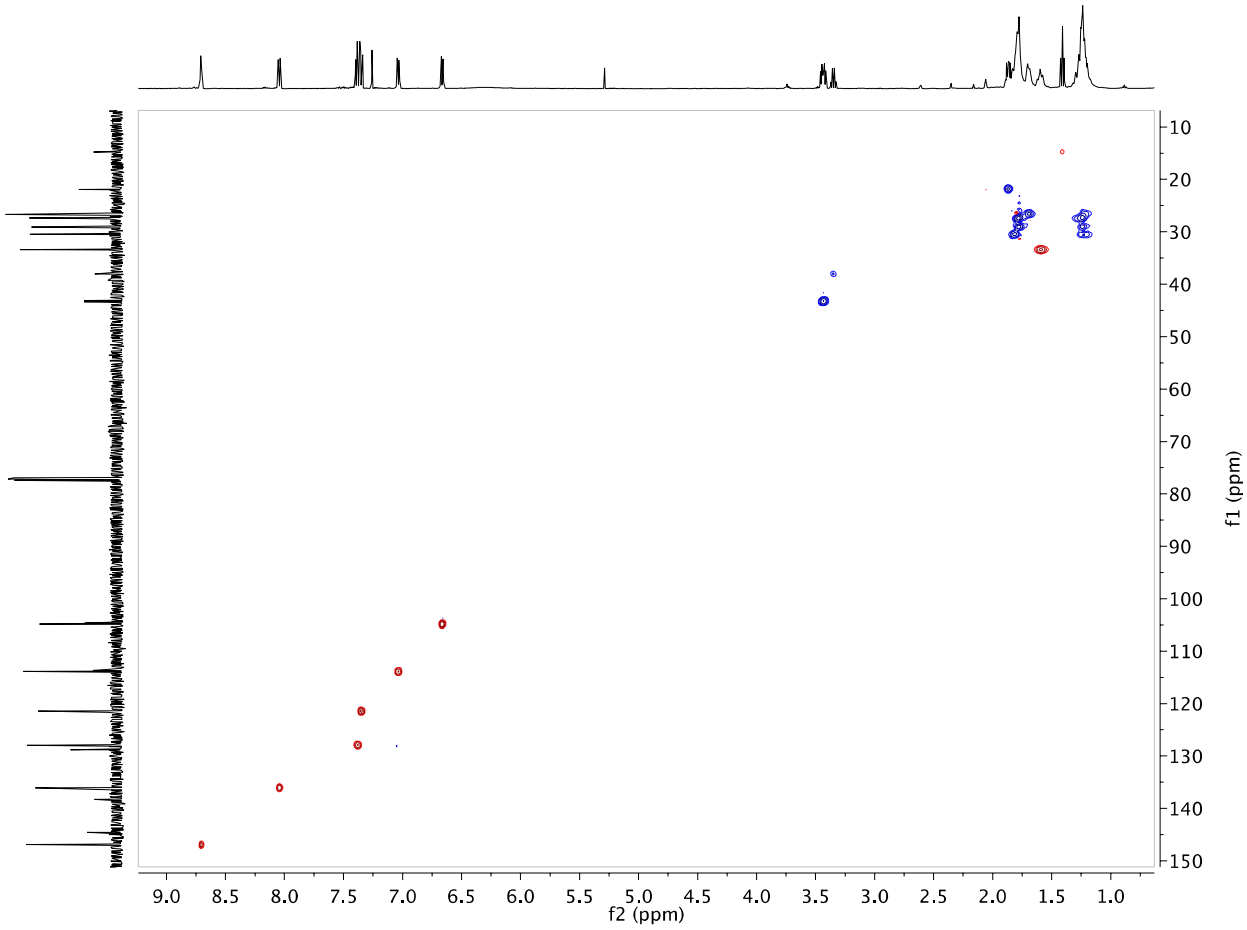

Figure S17. ^{1}H–^{13}C gHSQC spectrum of AQPNN-Cy **2b**

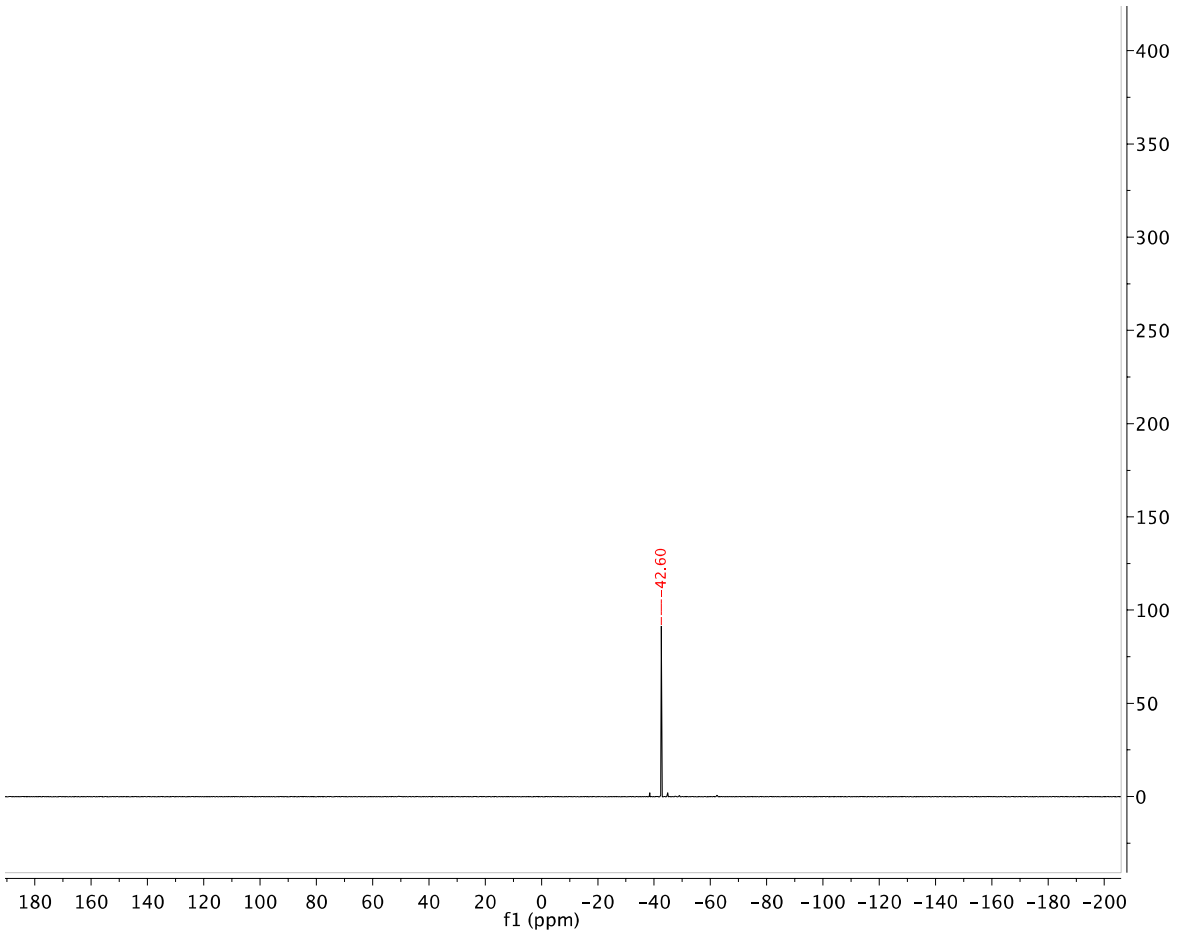

Figure S18. $^{31}P\{^{1}H\}$ NMR spectrum (202 MHz, $CDCl_3$) of AQPNN-^{i}Bu **2c**

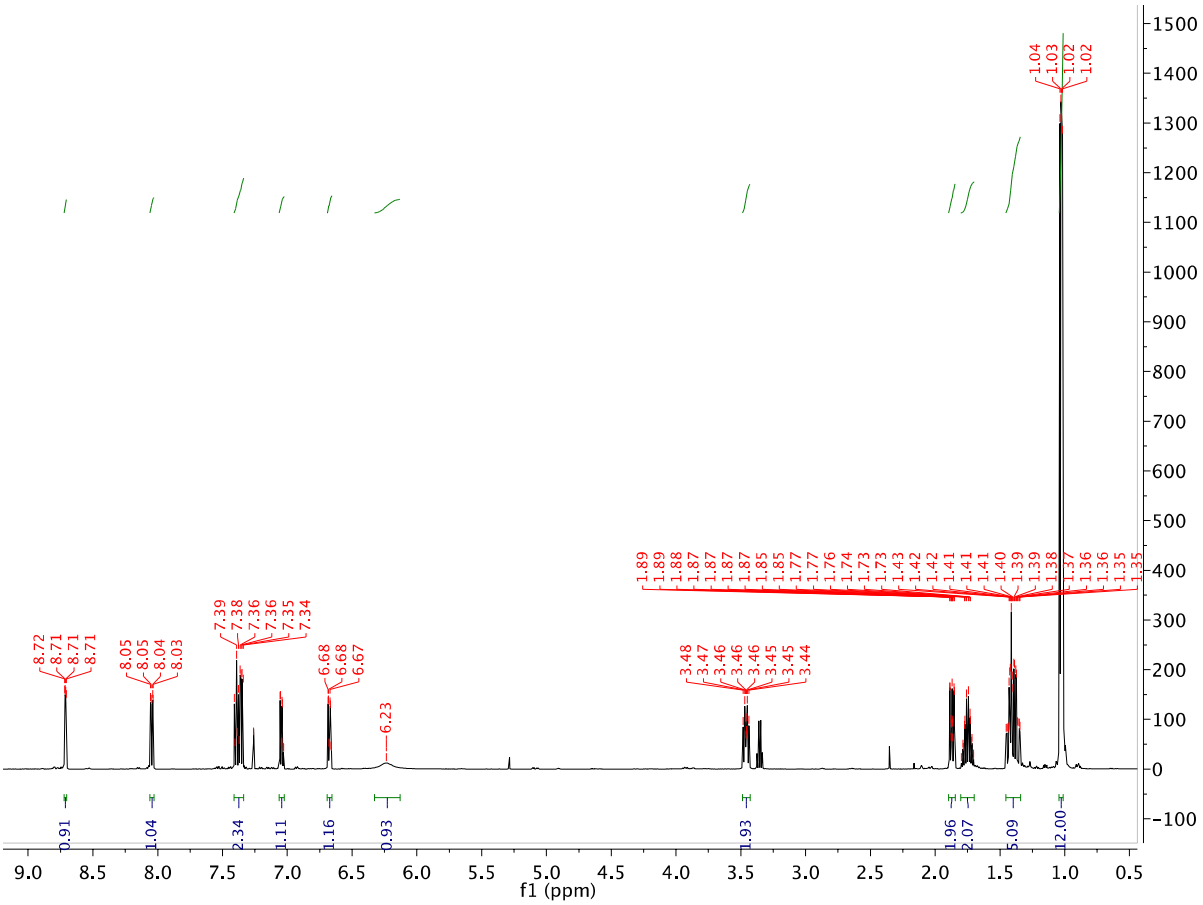

Figure S19. ^{1}H NMR spectrum (500 MHz, $CDCl_3$) of AQPNN-^{i}Bu **2c**

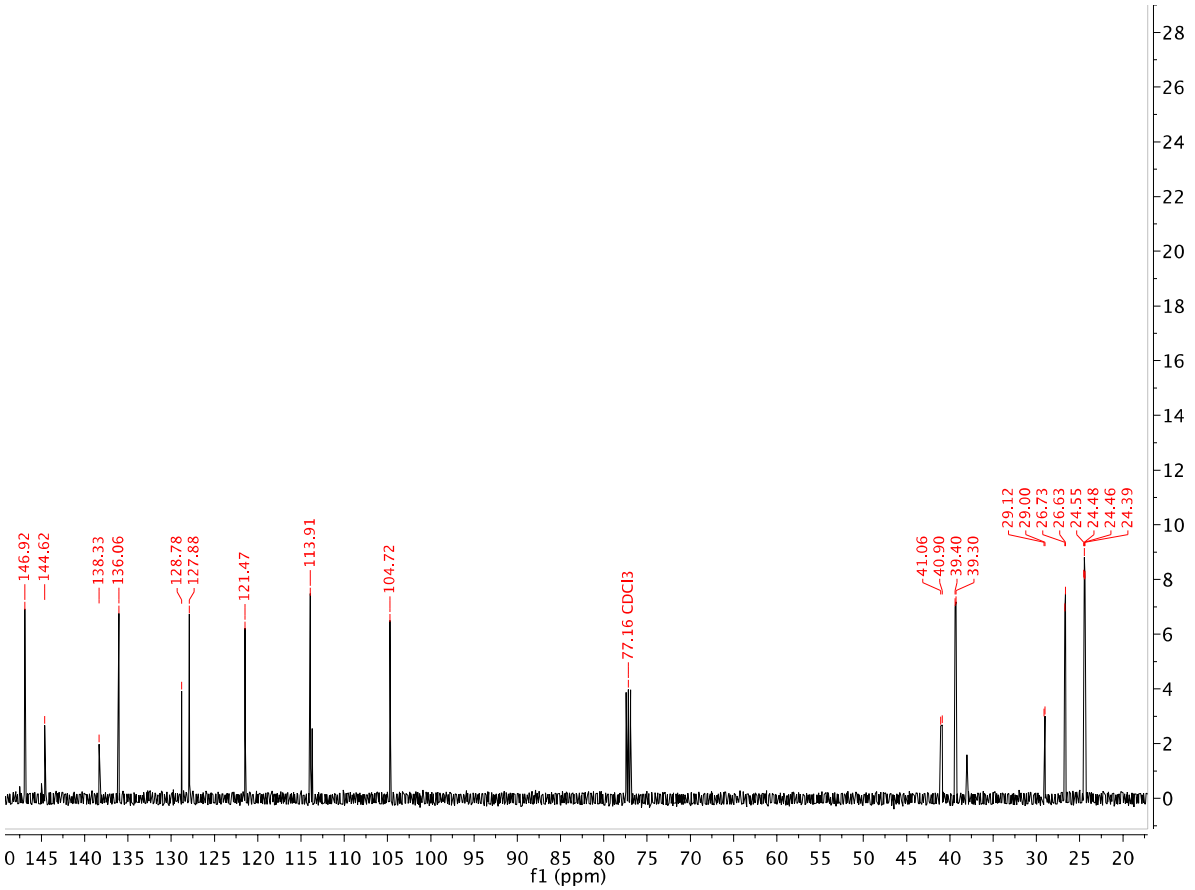

Figure S20. ^{13}C NMR spectrum (126 MHz, $CDCl_3$) of AQPNN-^{i}Bu **2c**

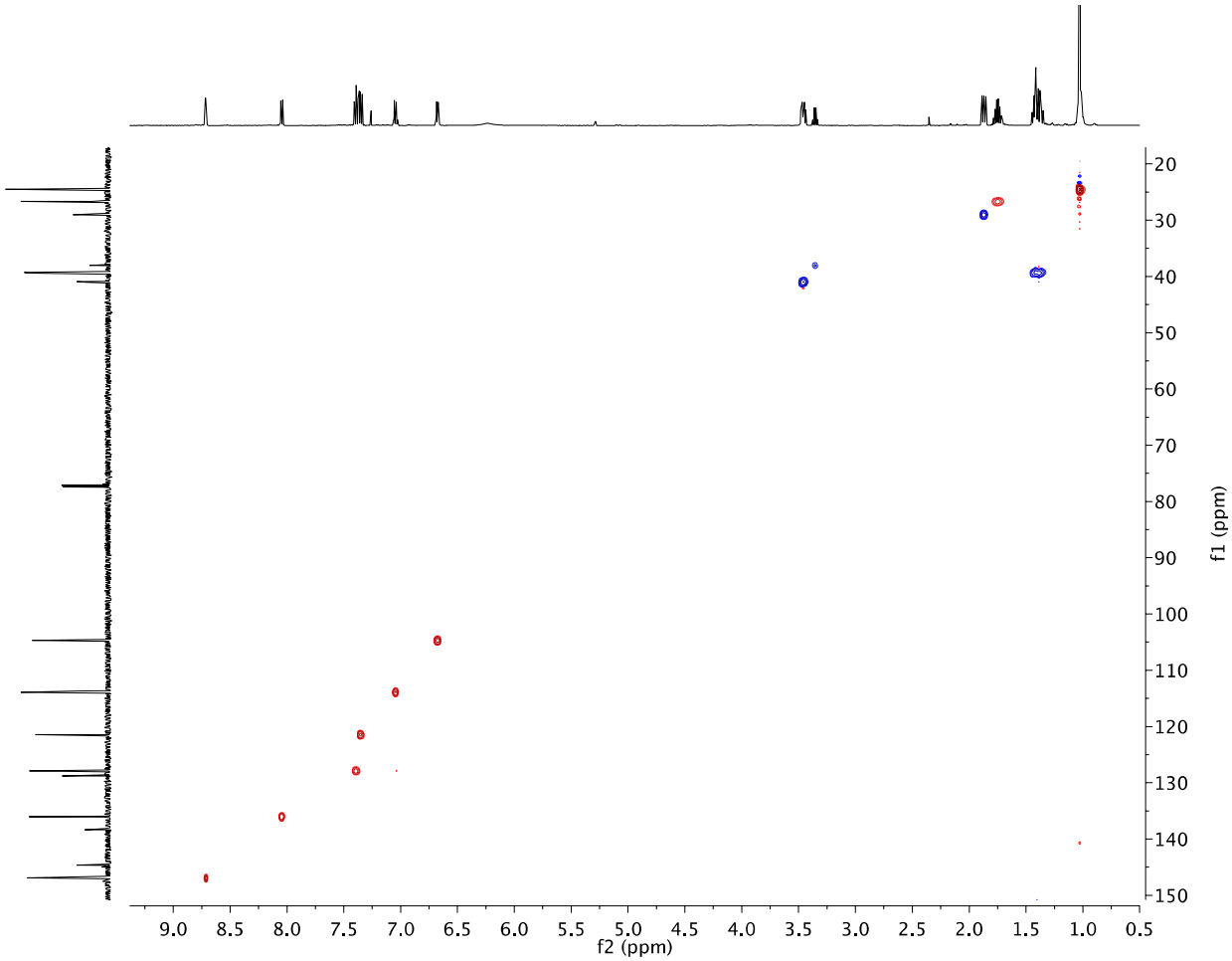

Figure S21. $^{1}H–^{13}C$ gHSQC spectrum of AQPNN-^{i}Bu **2c**

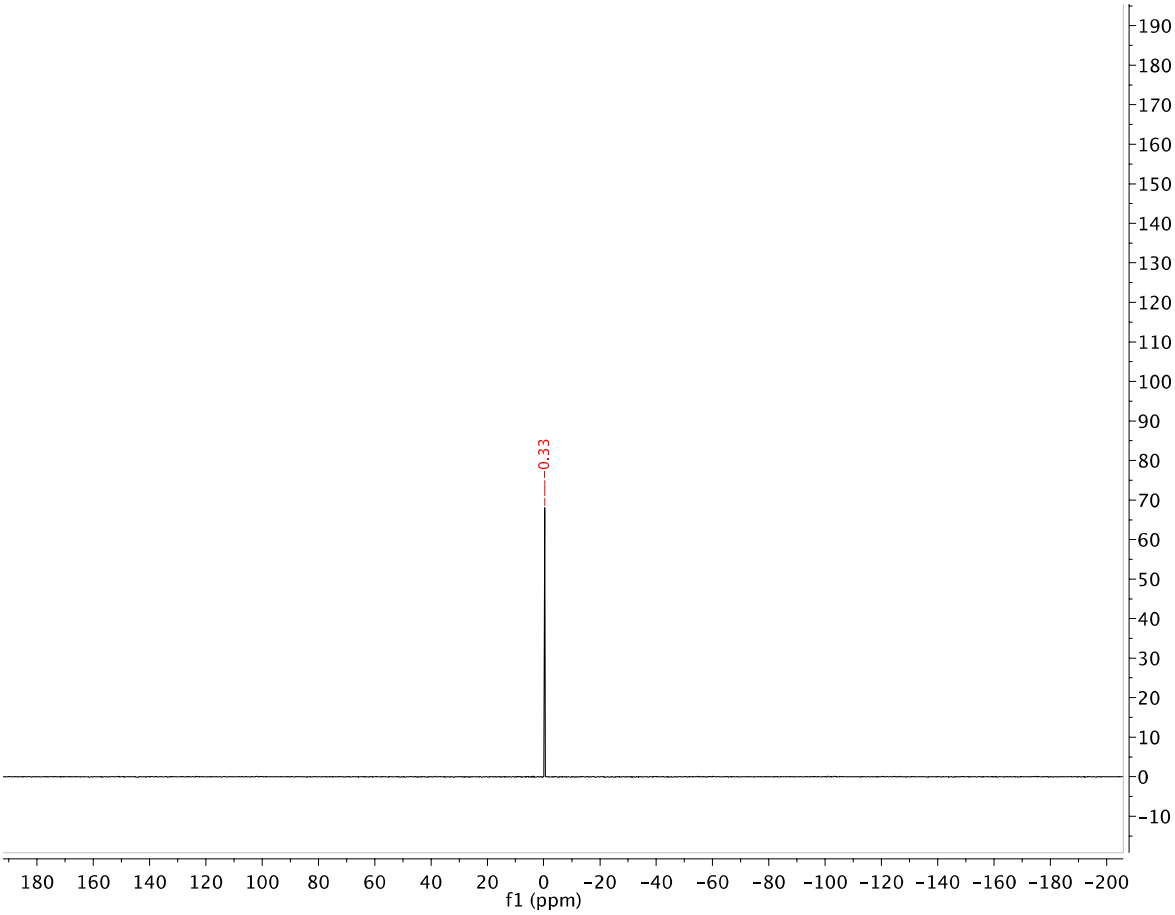

Figure S22. $^{31}P\{^{1}H\}$ NMR spectrum (202 MHz, $CDCl_3$) of AQPNN-^{i}Pr **2d**

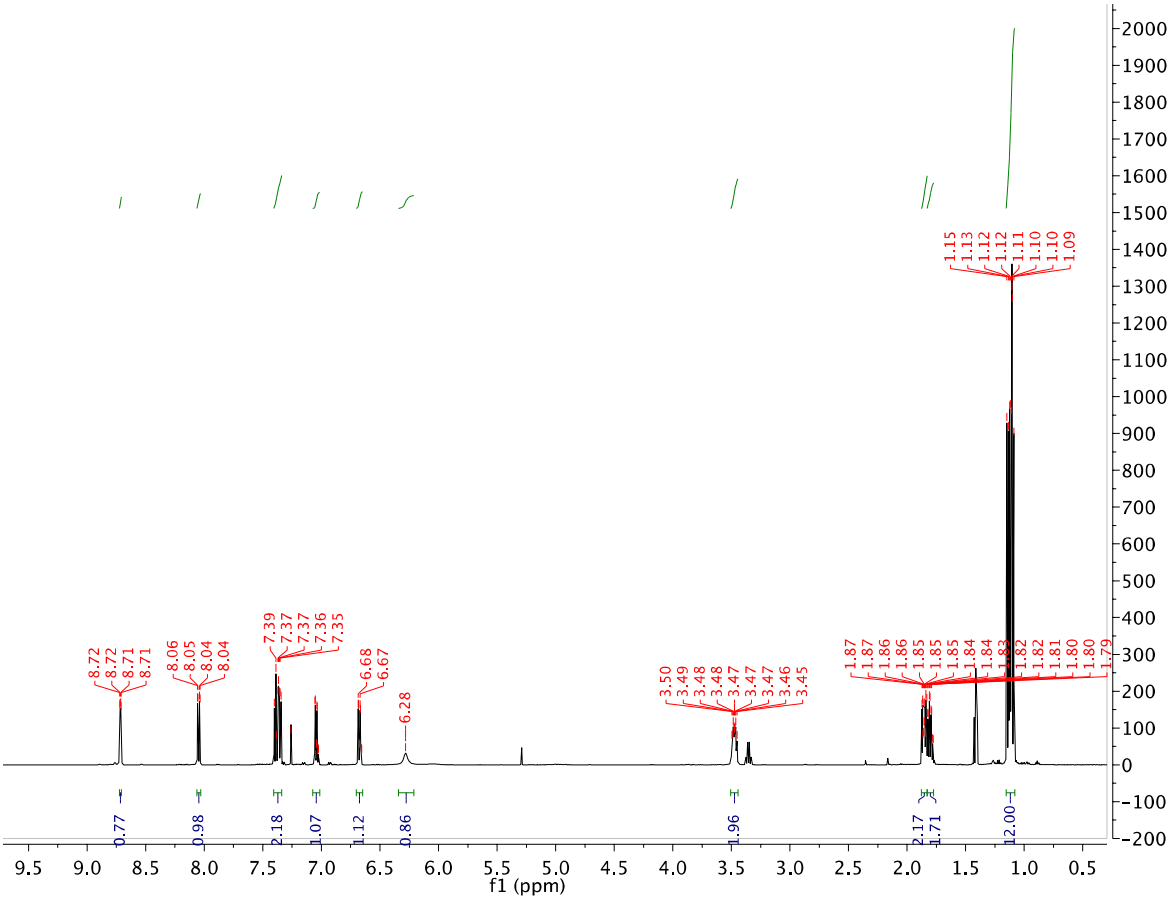

Figure S23. ^{1}H NMR spectrum (500 MHz, $CDCl_3$) of AQPNN-^{i}Pr **2d**

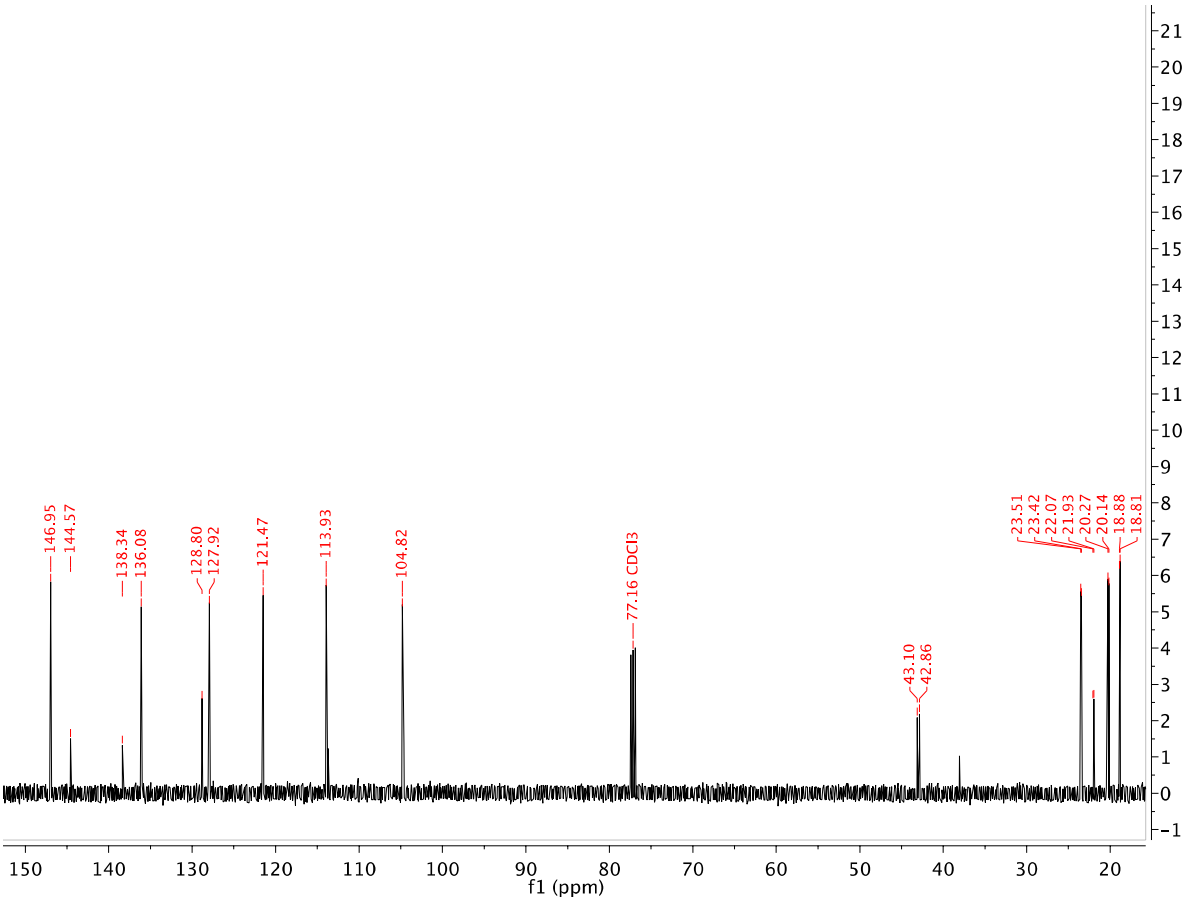

Figure S24. ^{13}C NMR spectrum (126 MHz, $CDCl_3$) of AQPNN-^{i}Pr **2d**

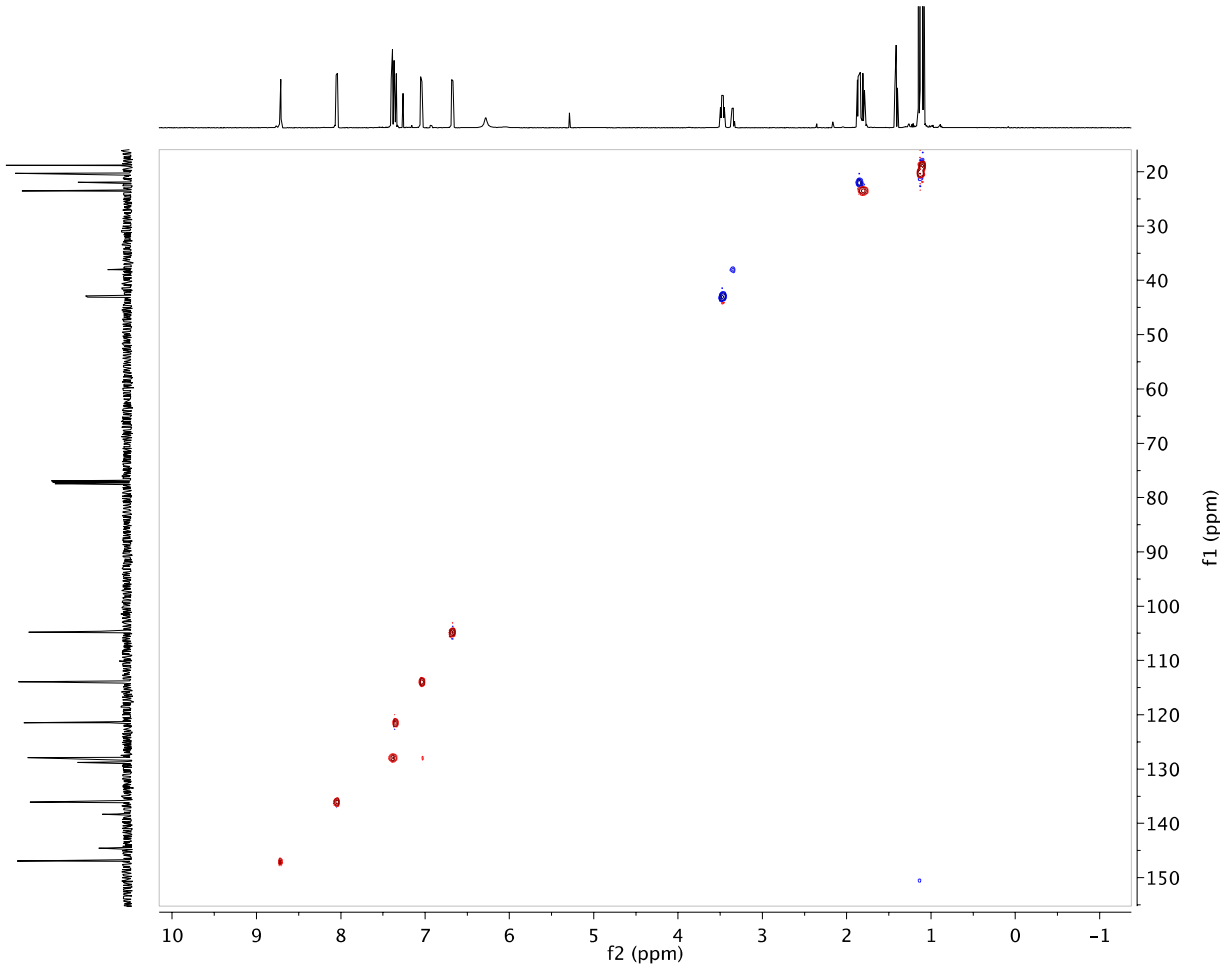

Figure S25. ^{1}H–^{13}C gHSQC spectrum of AQPNN-^{i}Pr **2d**

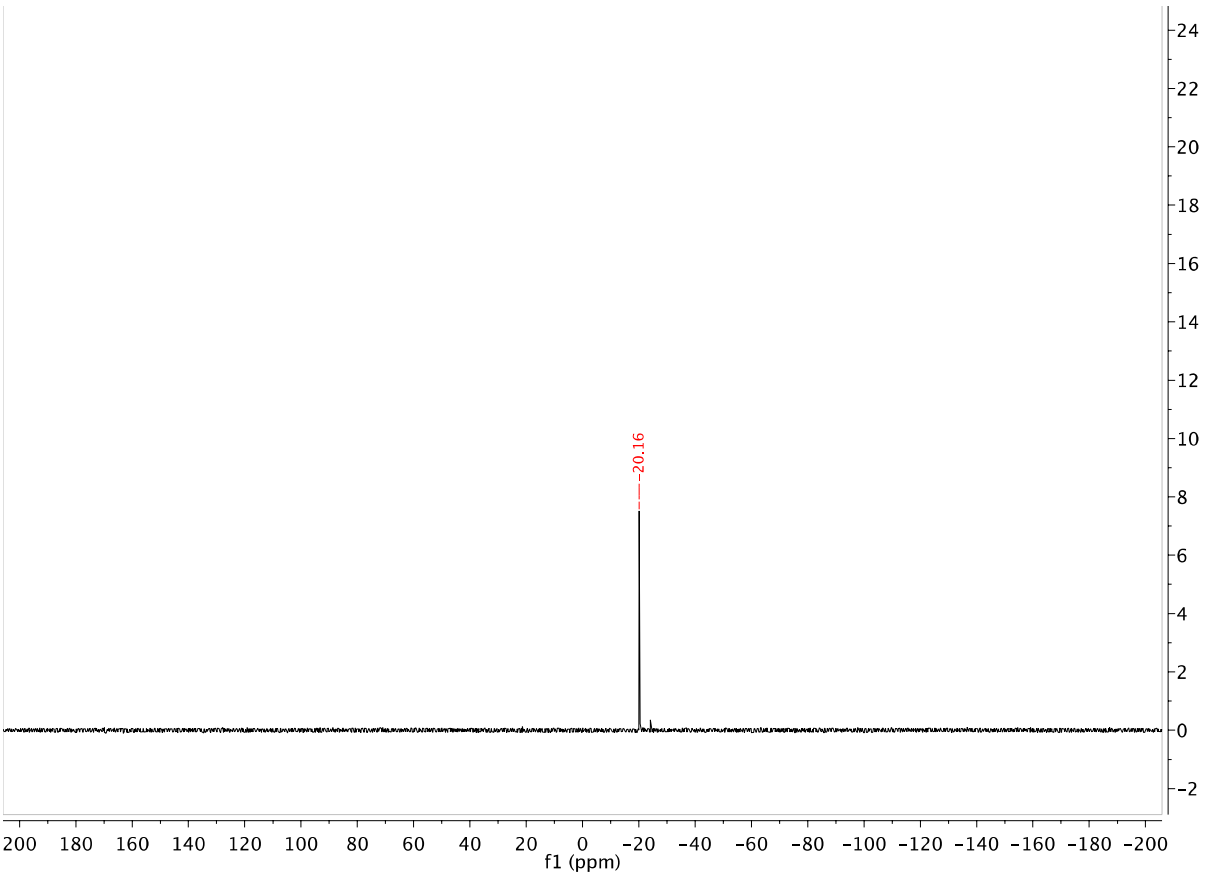

Figure S26. $^{31}P\{^{1}H\}$ NMR spectrum (202 MHz, $CDCl_3$) of P_2NN'-Ph **3a**

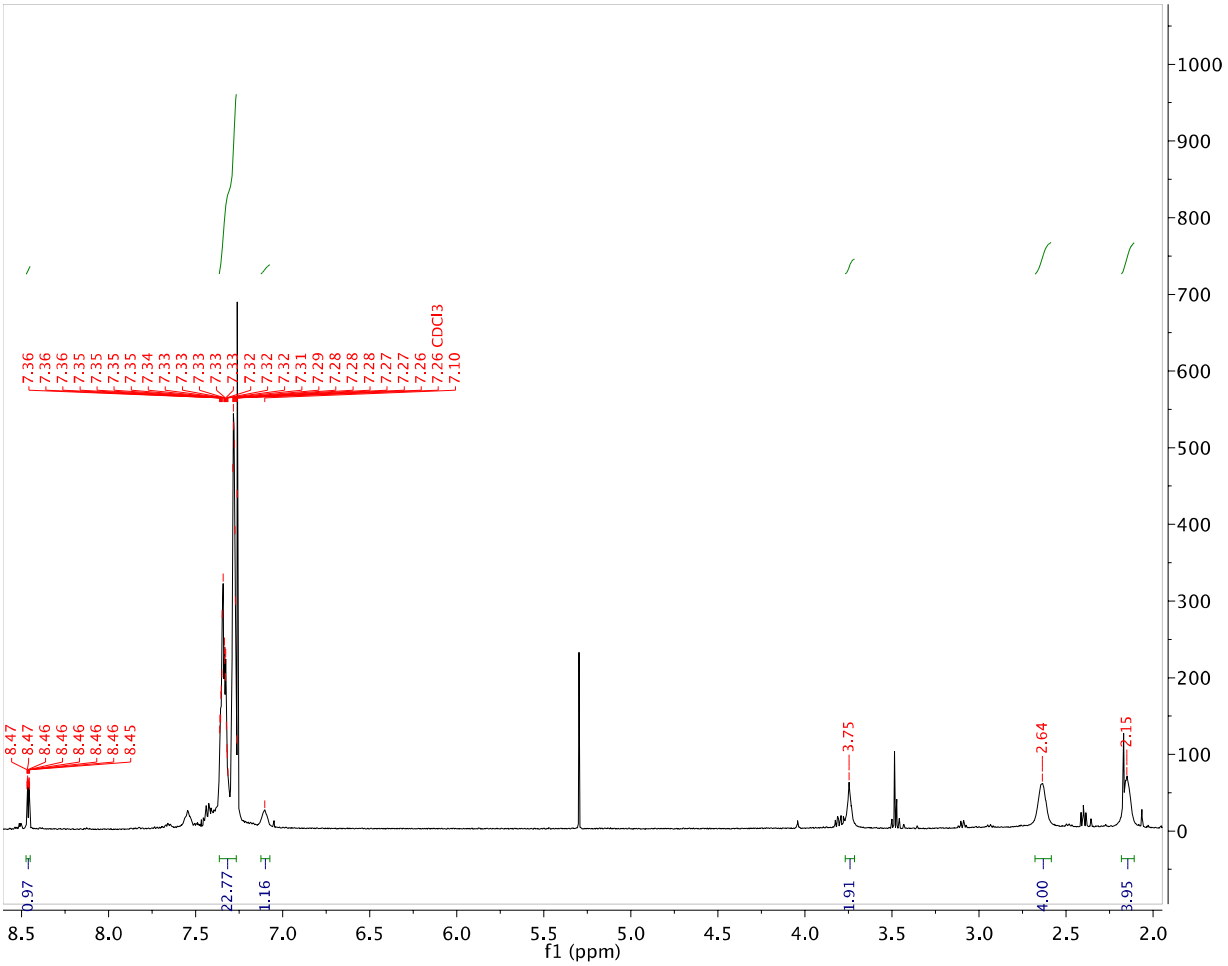

Figure S27. ^{1}H NMR spectrum (500 MHz, $CDCl_3$) of P_2NN'-Ph **3a**

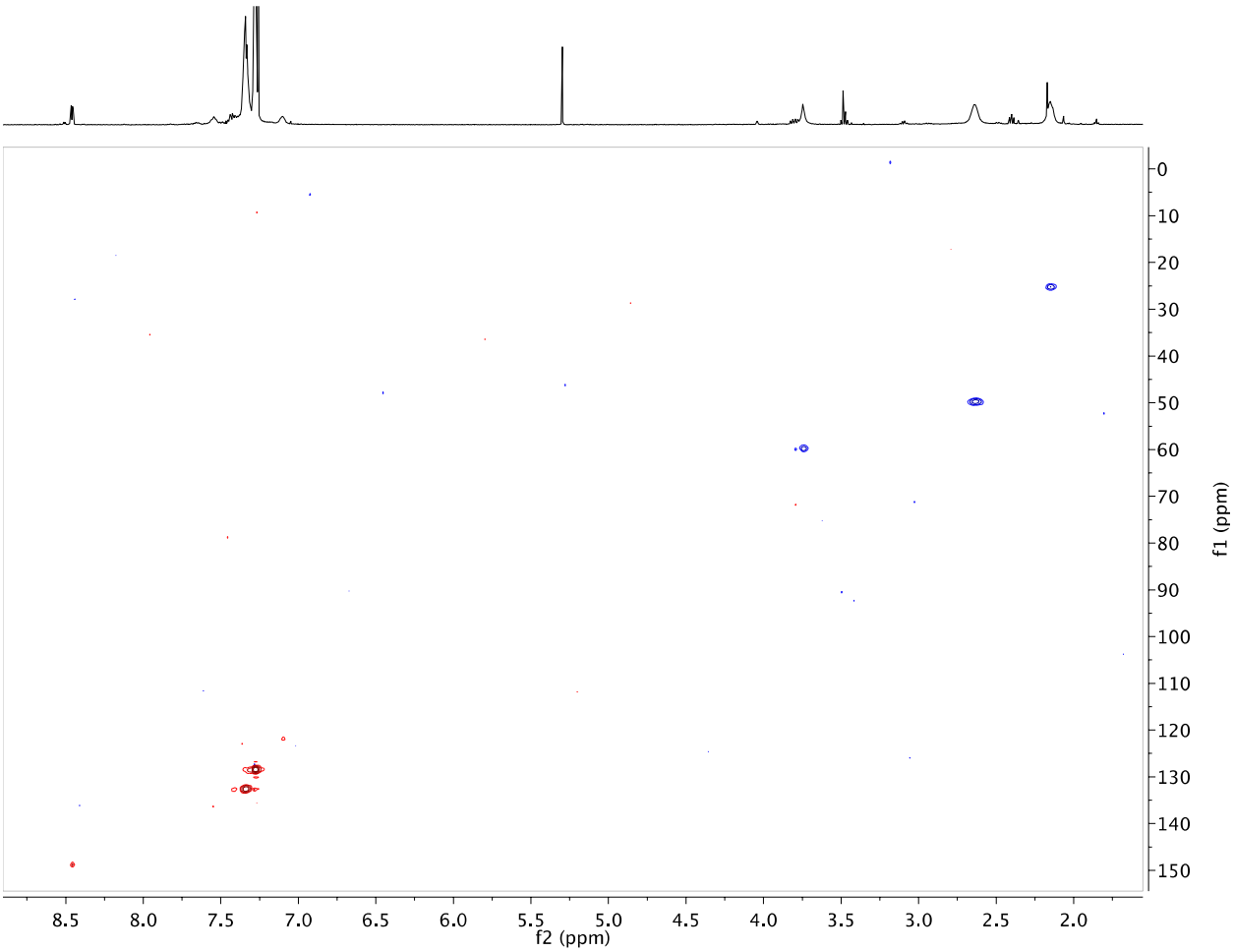

Figure #28. $^{1}H–^{13}C$ gHSQC spectrum of P_2NN'-Ph **3a**

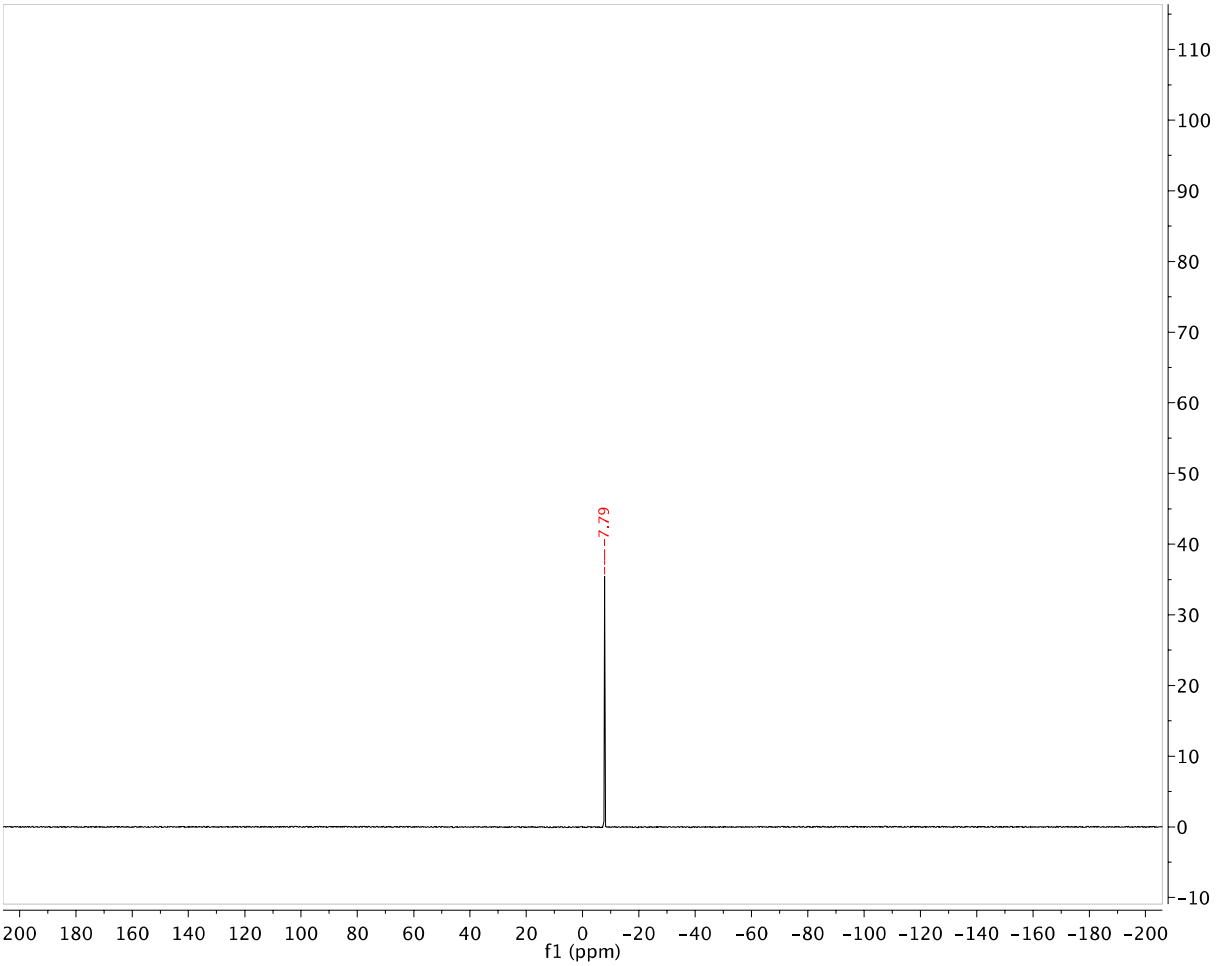

Figure S29. $^{31}P\{^{1}H\}$ NMR spectrum (202 MHz, $CDCl_3$) of P_2NN'-Cy **3b**

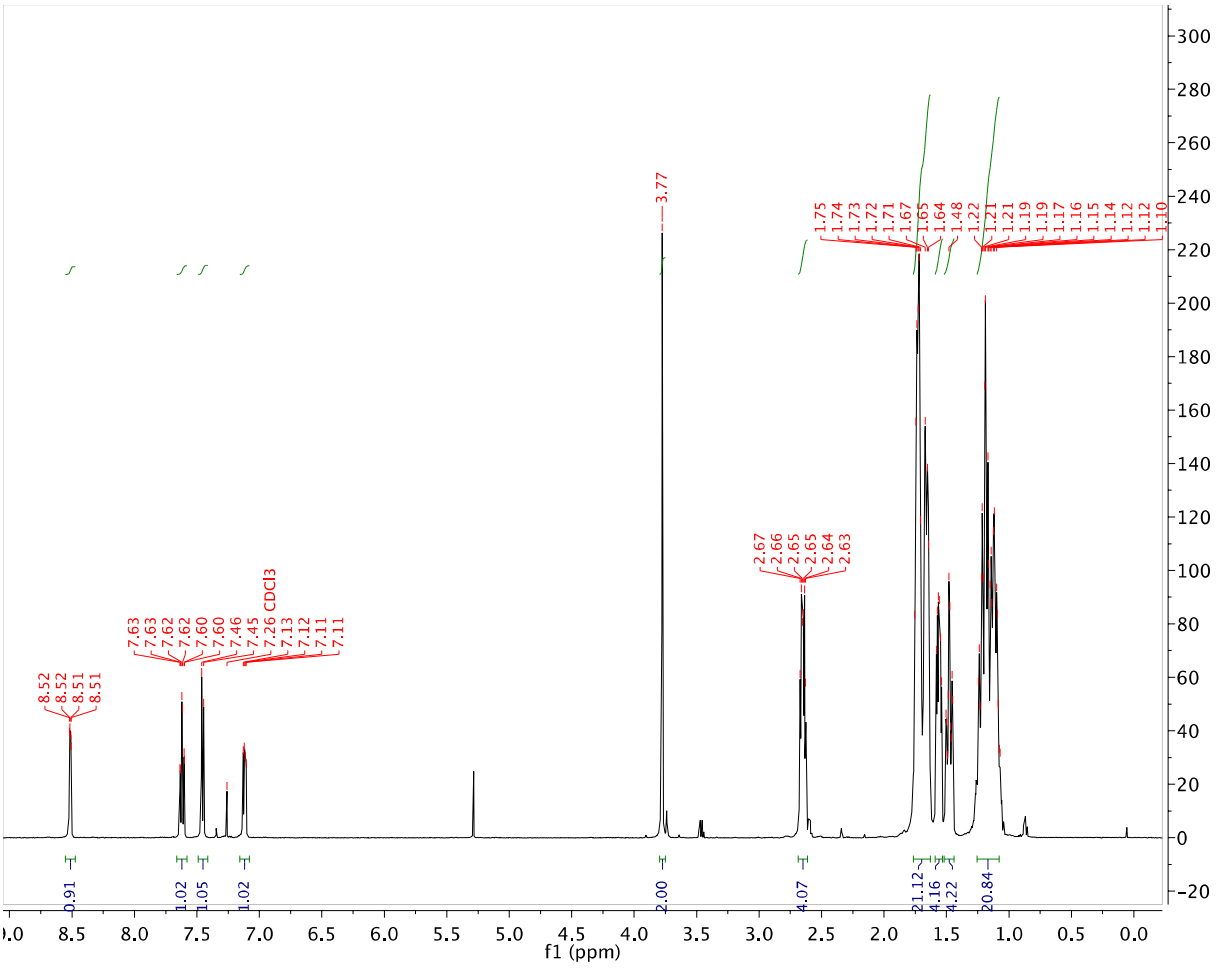

Figure S30. ^{1}H NMR spectrum (500 MHz, $CDCl_3$) of P_2NN'-Cy **3b**

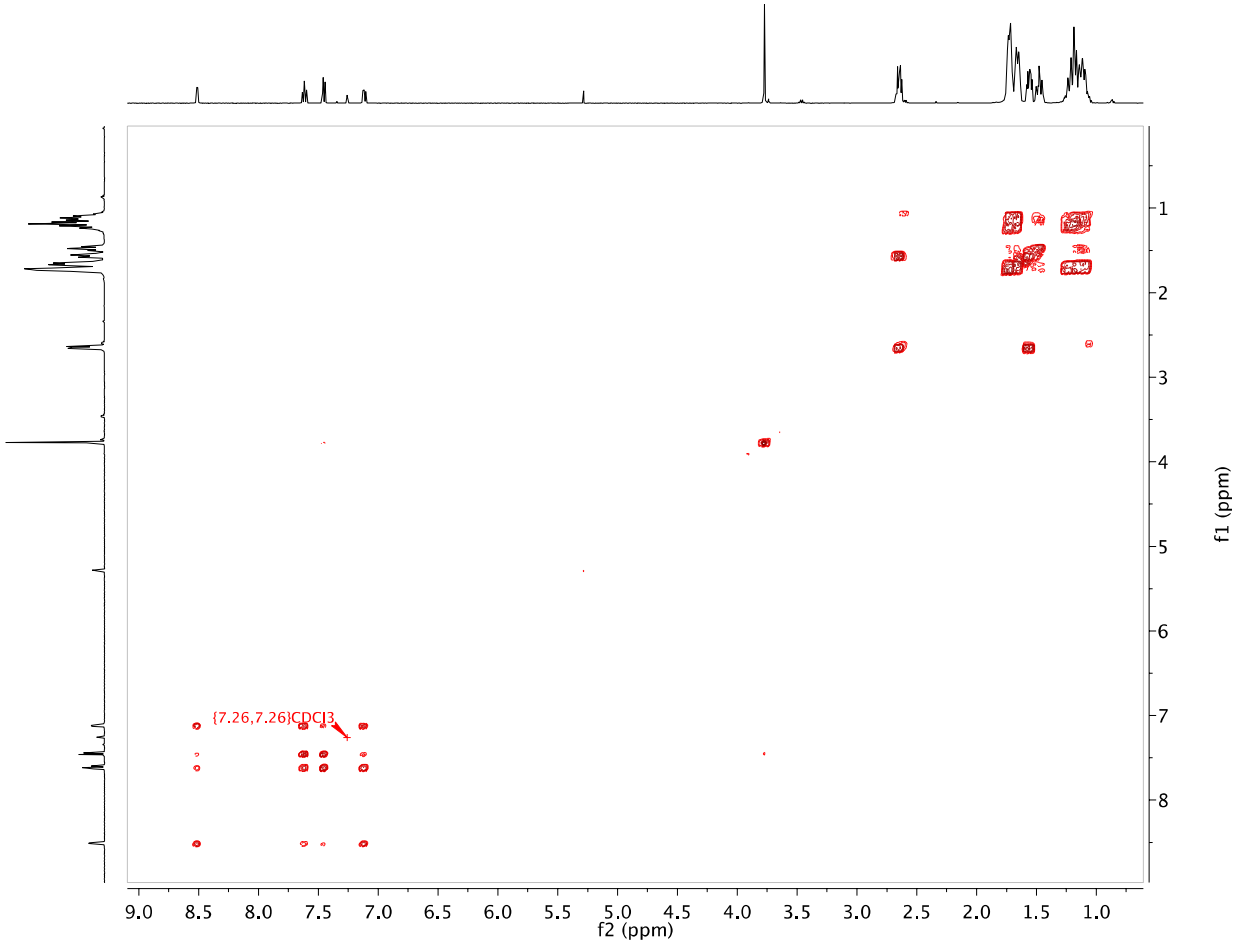

Figure #31. ^{1}H-^{1}H gCOSY spectrum (500 MHz, $CDCl_3$) of P_2NN'-Cy **3b**

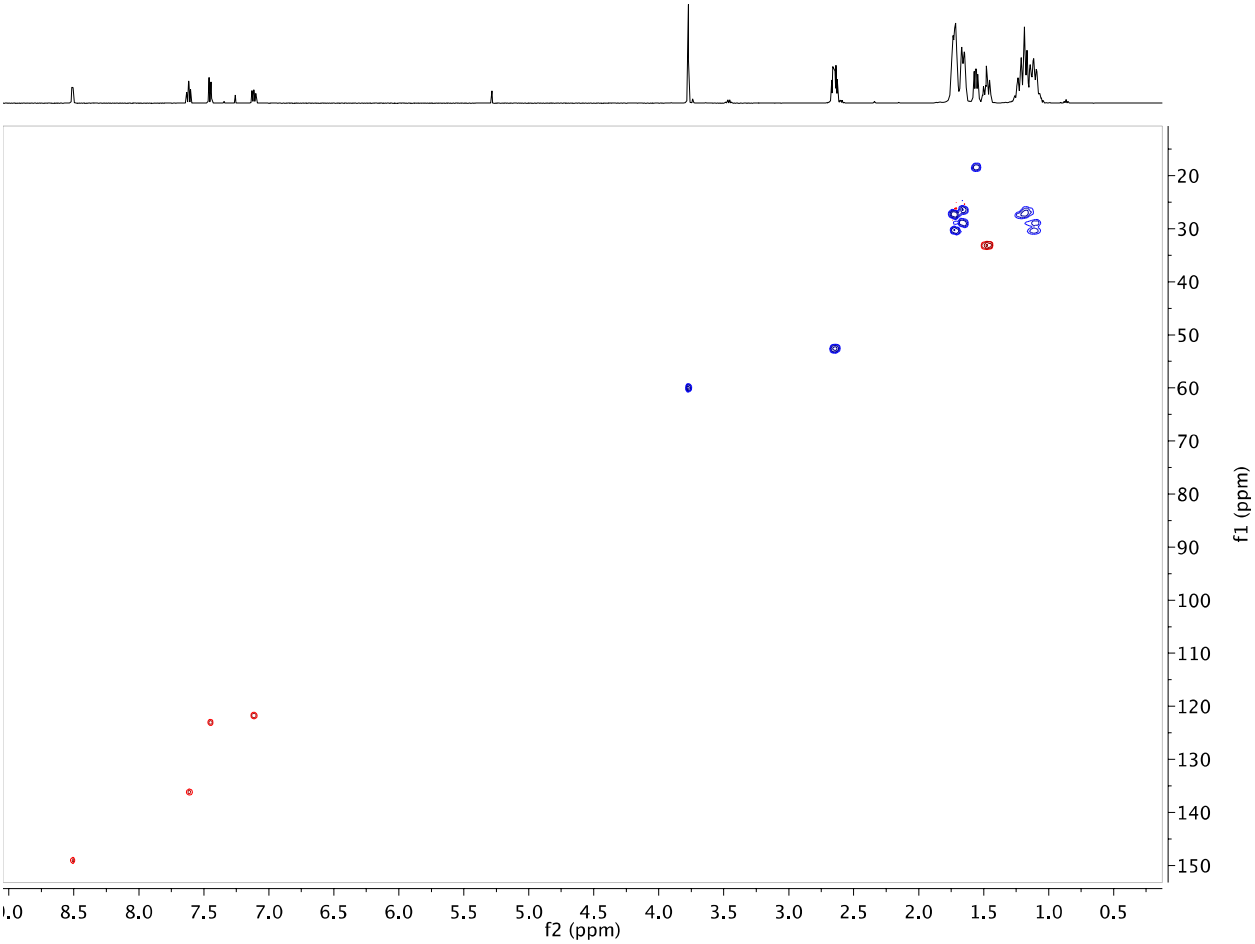

Figure S32. $^{1}H–^{13}C$ gHSQC spectrum of P_2NN'-Cy **3b**

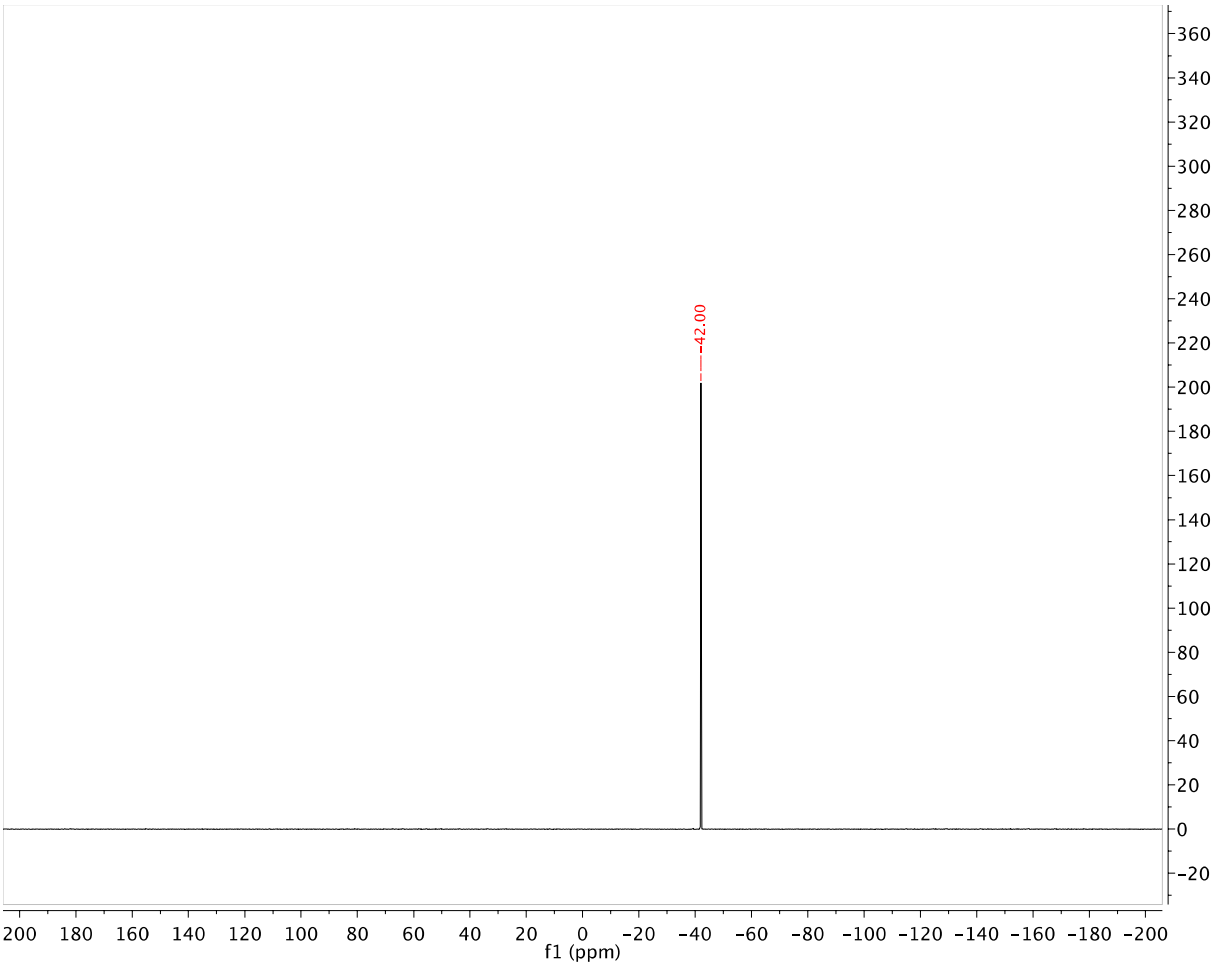

Figure S33. $^{31}P\{^{1}H\}$ NMR spectrum (202 MHz, $CDCl_3$) of P_2NN'-^{i}Bu **3c**

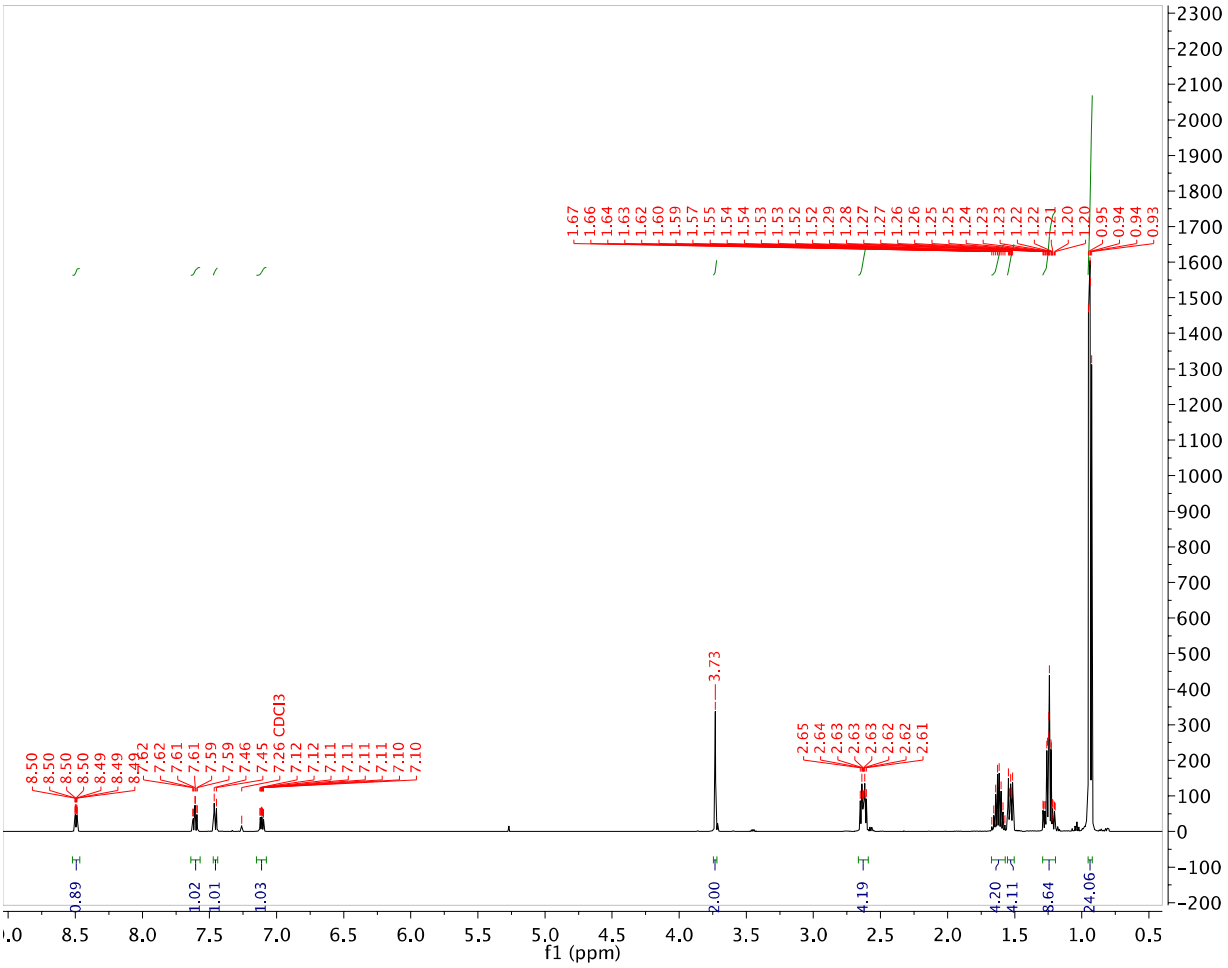

Figure S34. ^{1}H NMR spectrum (500 MHz, $CDCl_3$) of P_2NN'-^{i}Bu **3c**

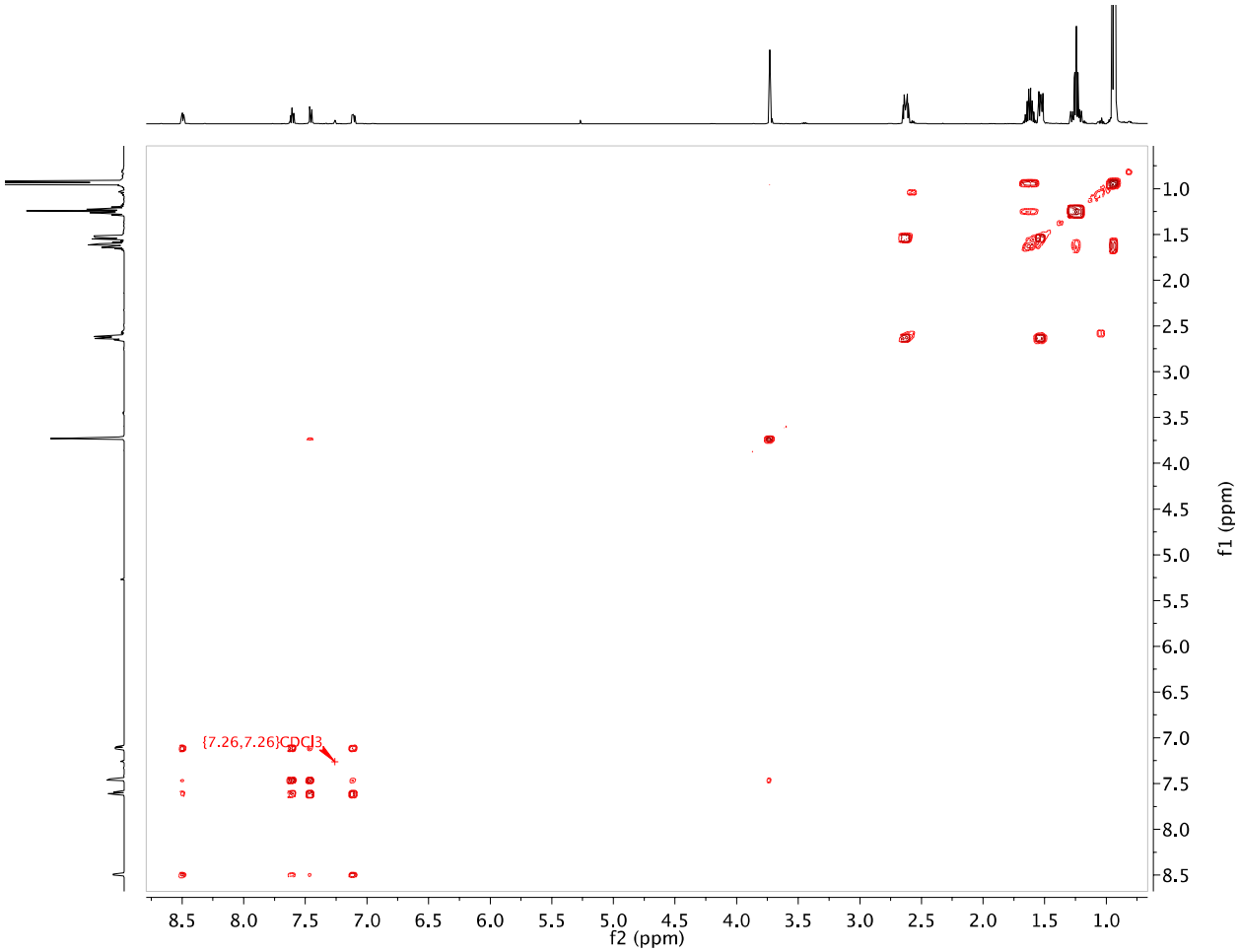

Figure S35. ^{1}H-^{1}H gCOSY spectrum (500 MHz, $CDCl_3$) of P_2NN'-^{i}Bu **3c**

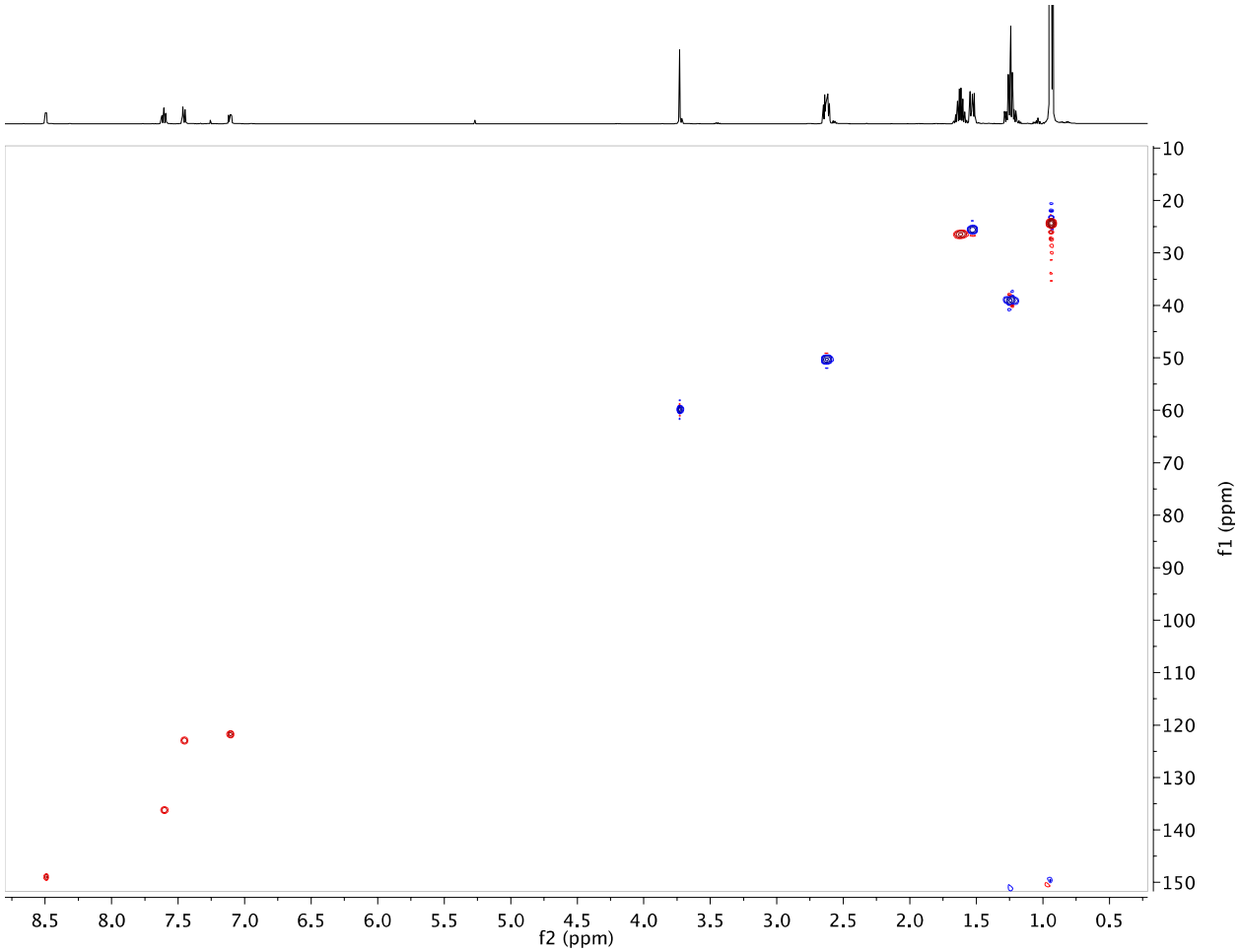

Figure S36. $^{1}H–^{13}C$ gHSQC spectrum of P_2NN'-^{i}Bu **3c**

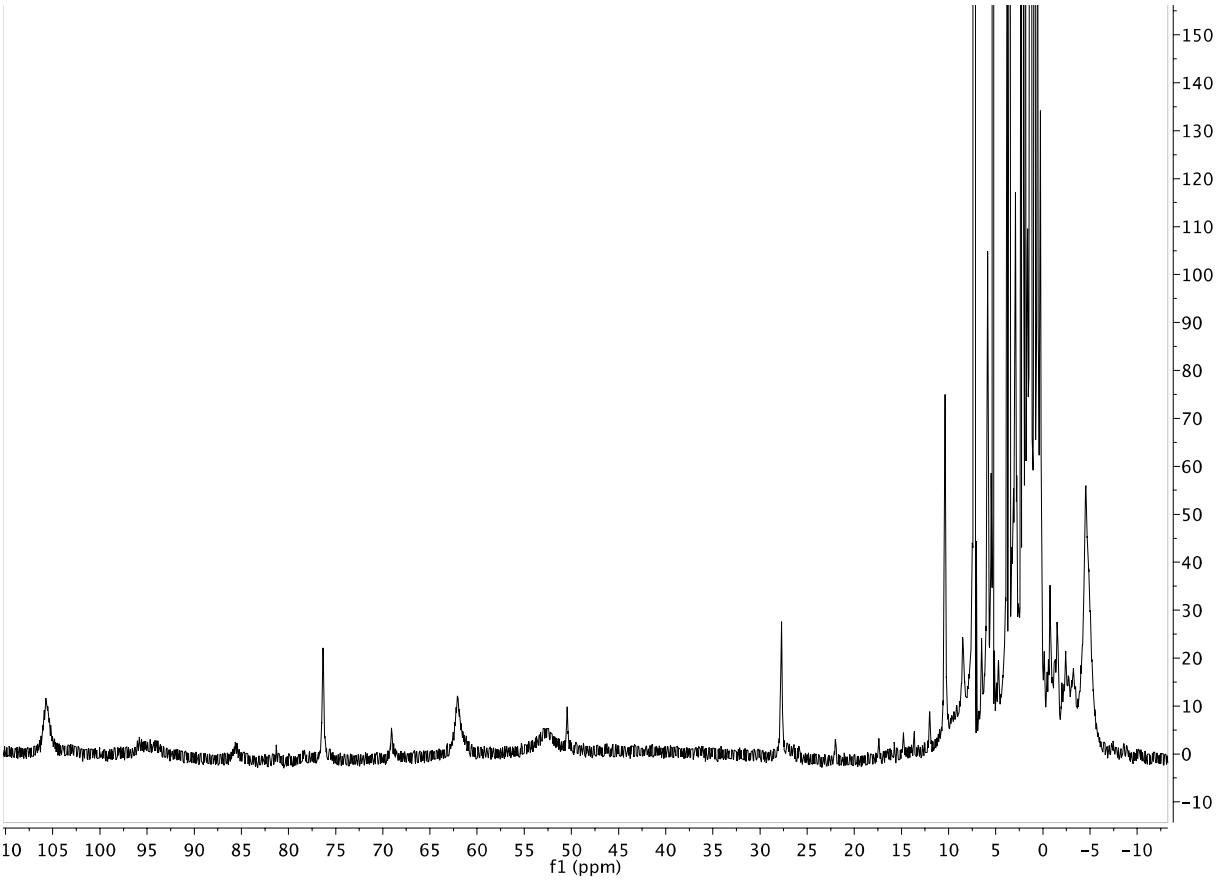

Figure S37. ^{1}H NMR spectrum (500 MHz, $CDCl_3$) of Co_2Cl_4(APyPNN-Cy)$_2$ **4**

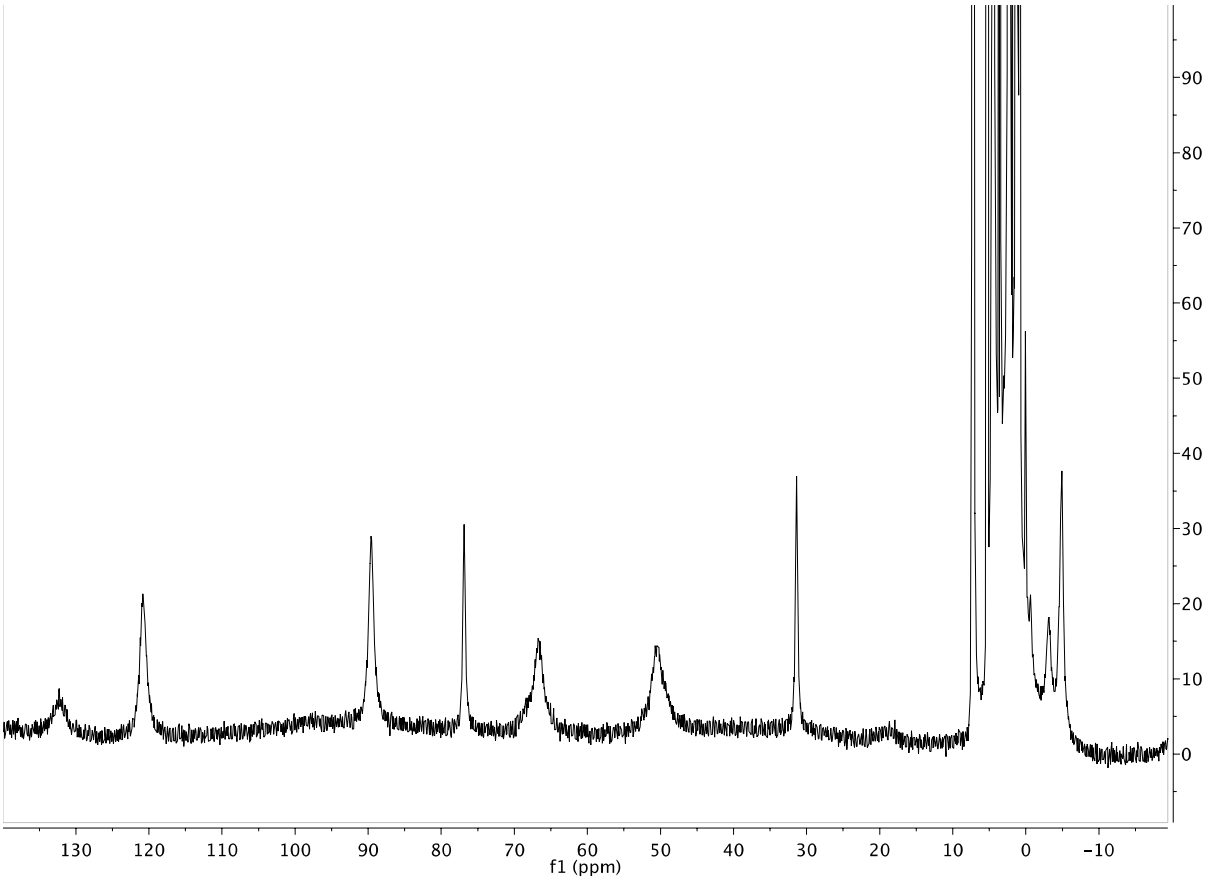

Figure S38. ^{1}H NMR spectrum (500 MHz, $CDCl_3$) of Co_2Cl_4(APyPNN-^{i}Bu)$_2$ **5**

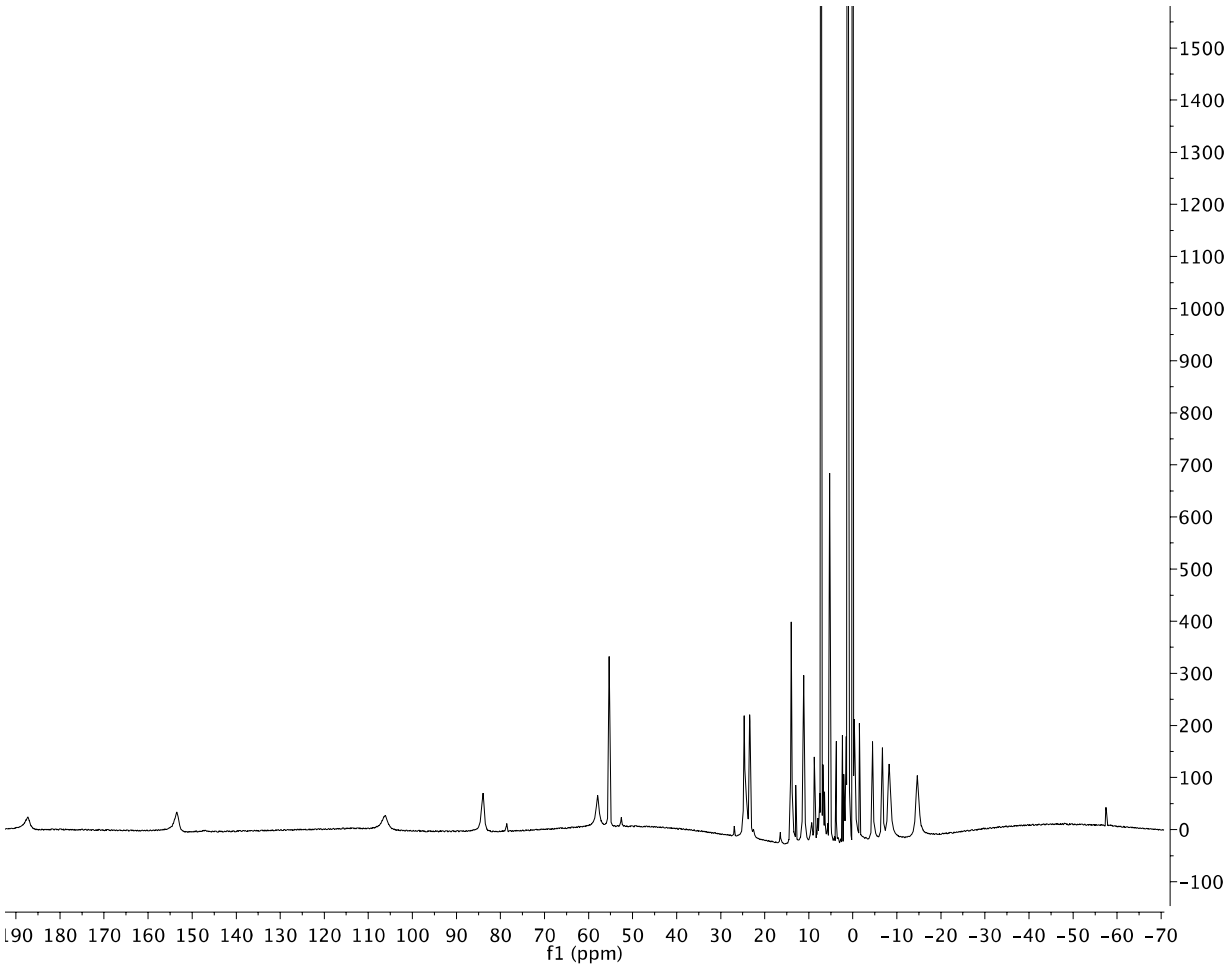

Figure S39. ^{1}H NMR spectrum (500 MHz, $CDCl_3$) of $CoCl_2$(AQPNN-Ph) **6**

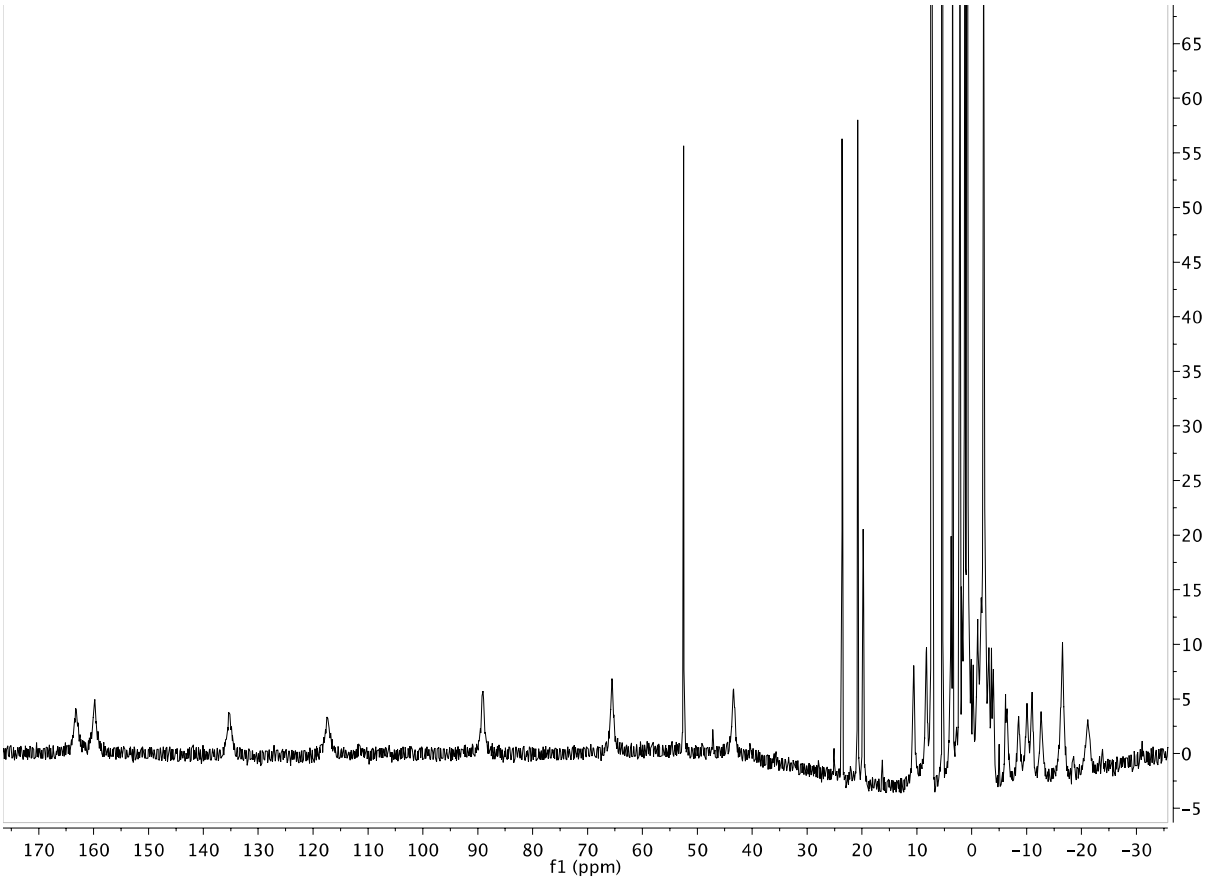

Figure S40. ^{1}H NMR spectrum (500 MHz, $CDCl_3$) of $CoCl_2$(AQPNN-Cy) **7**

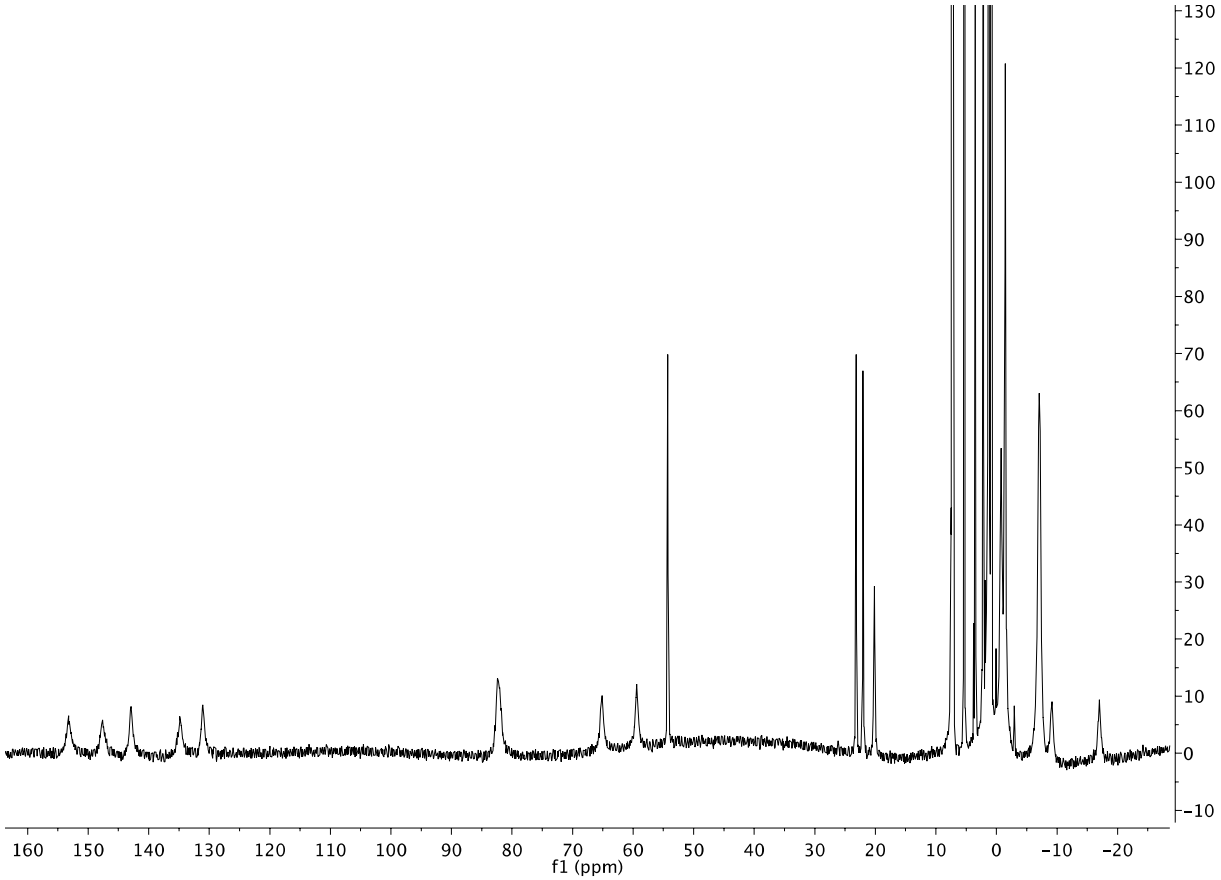

Figure S41. ^{1}H NMR spectrum (500 MHz, $CDCl_3$) of $CoCl_2$(AQPNN-^{i}Bu) **8**

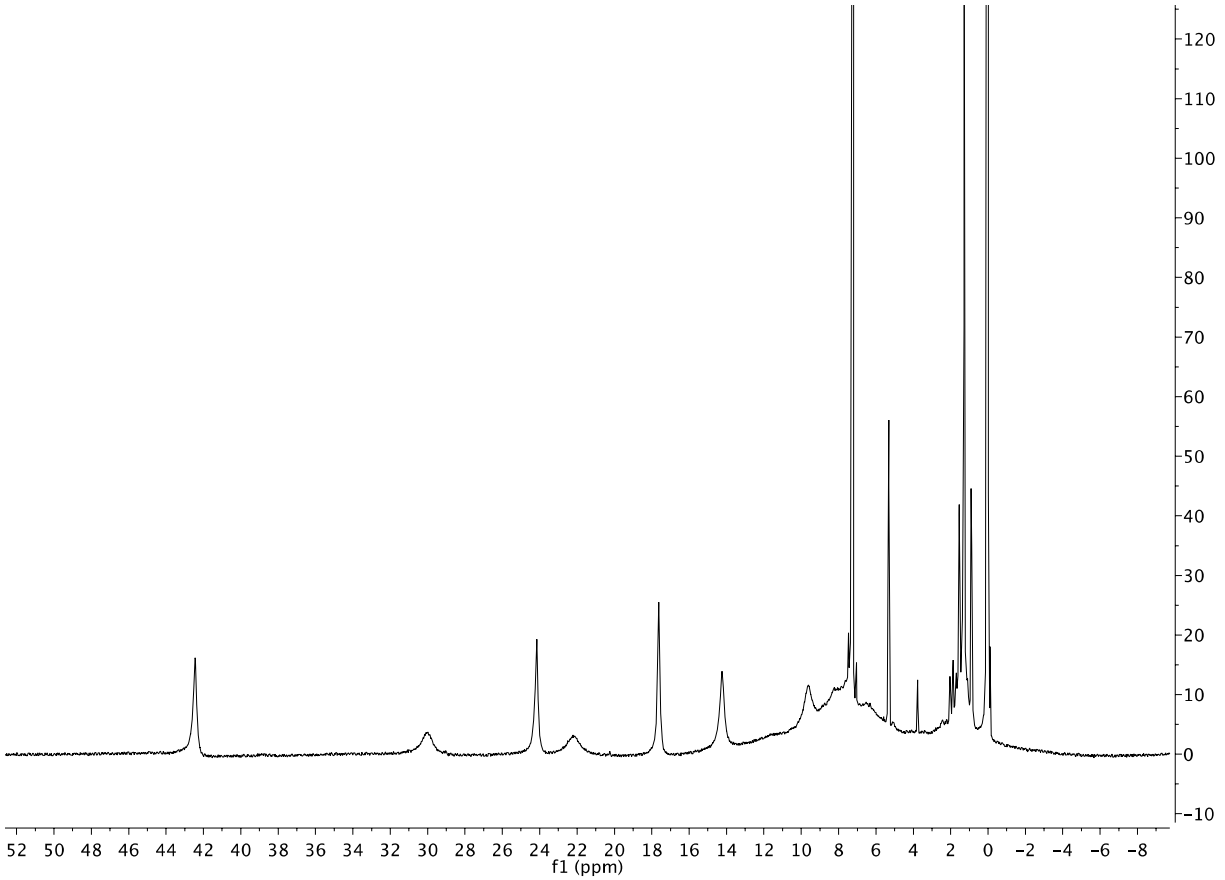

Figure S42. ^{1}H NMR spectrum (500 MHz, $CDCl_3$) of $FeCl_2$(AQPNN-^{i}Pr) **9**

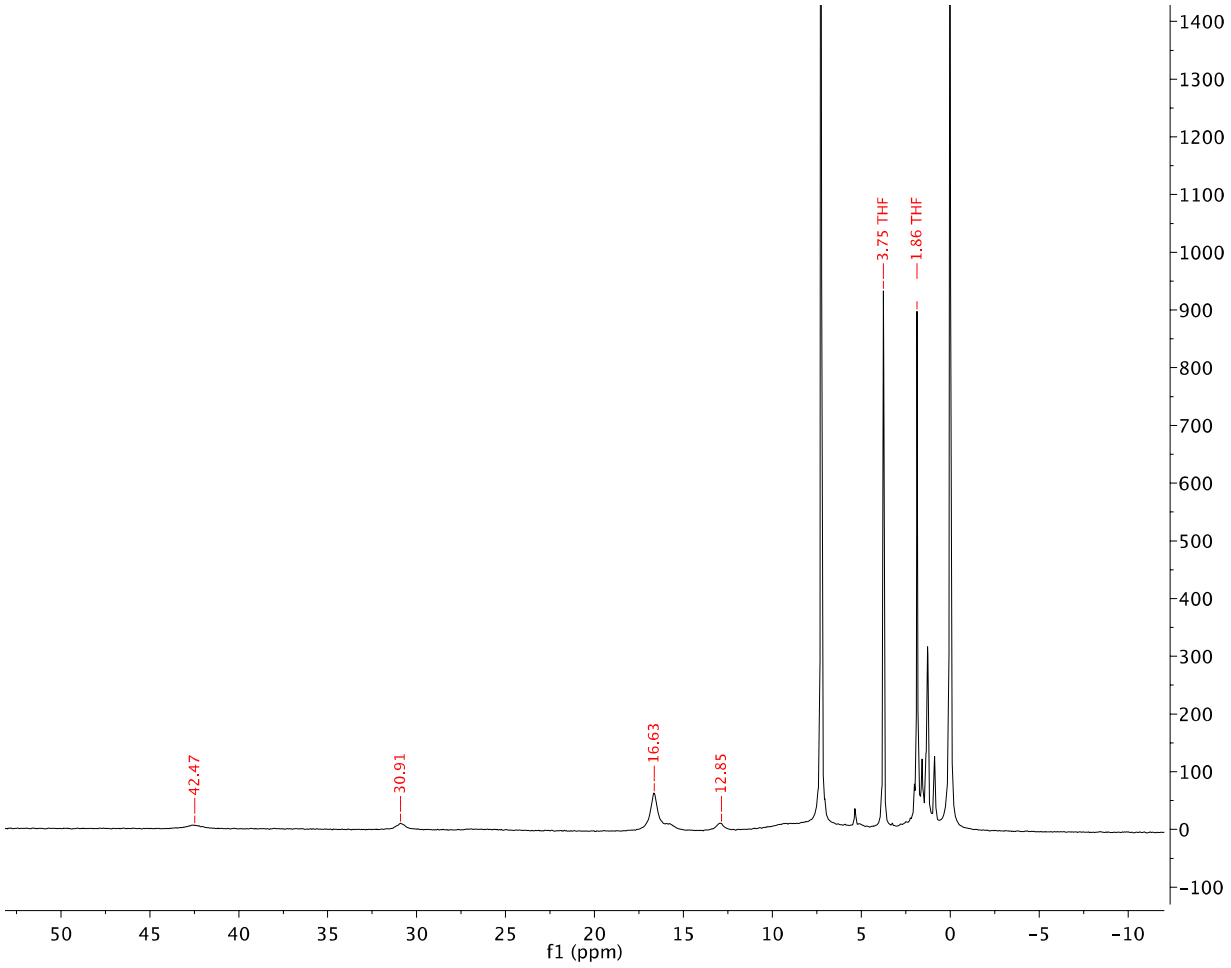

Figure S43. ^{1}H NMR spectrum (500 MHz, $CDCl_3$) of $[FeCl_2(AQPNN\text{-}Ph)]_2$ **10**

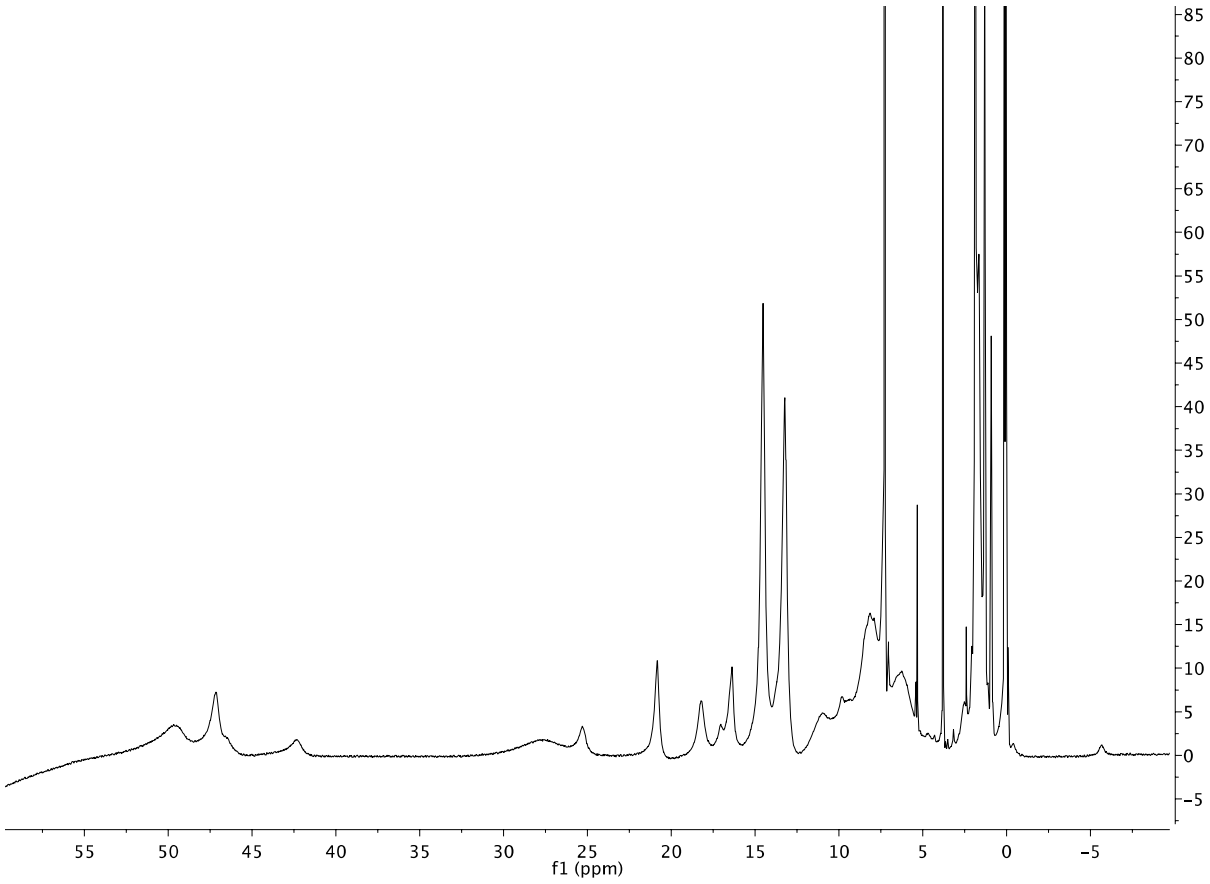

Figure S44. ^{1}H NMR spectrum (500 MHz, $CDCl_3$) of $FeCl_2(P_2NN')$ **11**

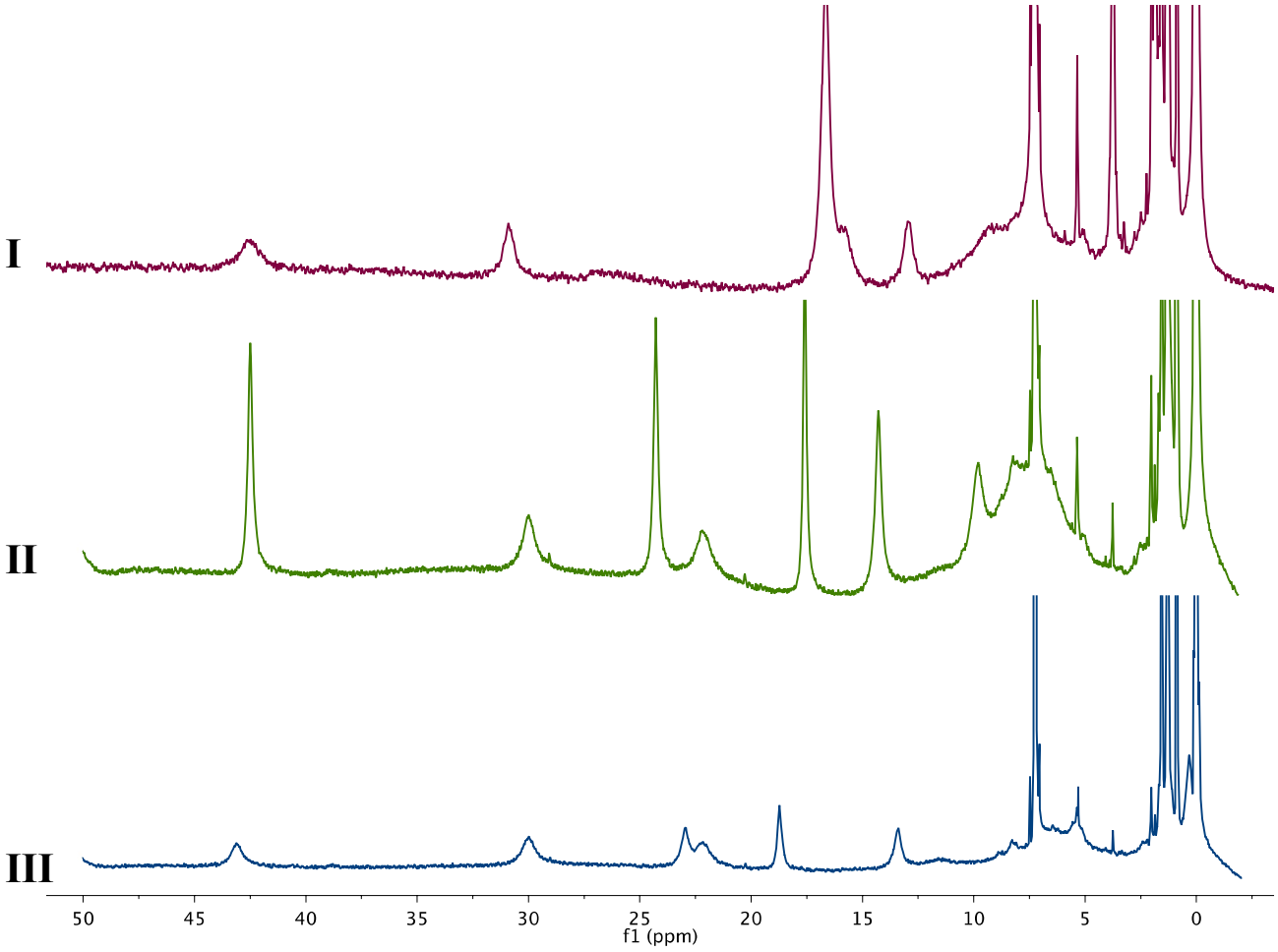

Figure S45. ^{1}H NMR spectrum (500 MHz, $CDCl_3$) of **10** (**I**), **9** (**II**), and **9** at half concentration (**III**).[a]

[a]Evans method for **9** was also conducted on 0.002 and 0.004 M solutions however no change in the μ_{eff} value was observed.

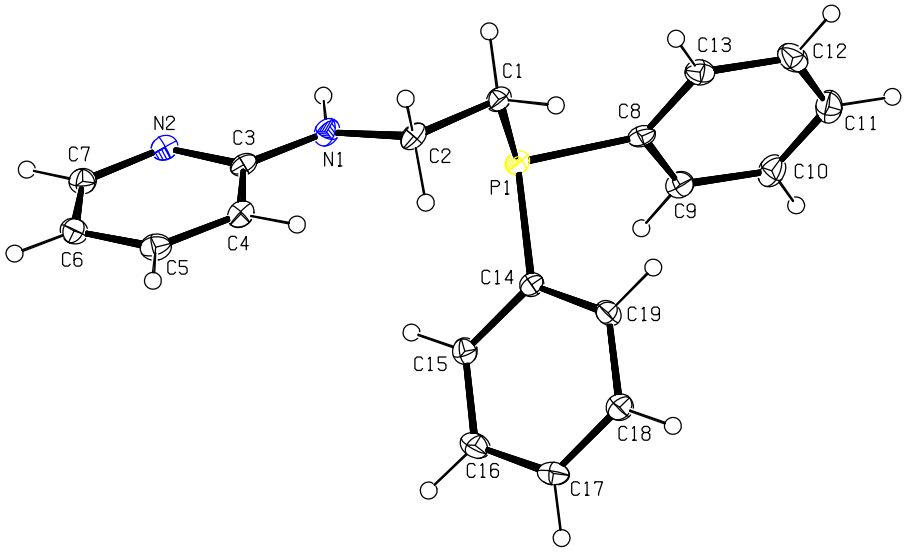

Figure S46. X-ray structure of APyPNN-Ph **1a**. Ellipsoids are shown at 50% probability. Selected bond lengths (Å) and angles (deg): P(1)-C(8) 1.838(2), P(1)-C(14) 1.843(2), P(1)-C(1) 1.843(2), N(1)-C(3) 1.366(3), N(1)-C(2) 1.456(3), C(8)-P(1)-C(14) 98.95(9), C(8)-P(1)-C(1) 102.54(10), C(14)-P(1)-C(1) 100.92(9), C(3)-N(1)-C(2) 120.71(18).

Table S1. Crystal data and structure refinement for **1a**.

Identification code	d1829a_a	
Empirical formula	C19 H19 N2 P	
Formula weight	306.33	
Temperature	150(2) K	
Wavelength	0.71073 Å	
Crystal system	Monoclinic	
Space group	$P2_1/c$	
Unit cell dimensions	a = 18.4650(19) Å	a= 90°.
	b = 5.4113(5) Å	b= 116.474(3)°.
	c = 17.7373(18) Å	g = 90°.
Volume	1586.5(3) $Å^3$	
Z	4	
Density (calculated)	1.283 Mg/m^3	
Absorption coefficient	0.171 mm^{-1}	
F(000)	648	
Crystal size	0.190 x 0.150 x 0.100 mm^3	
Theta range for data collection	2.298 to 27.605°.	
Index ranges	-23<=h<=23, -7<=k<=7, -23<=l<=20	
Reflections collected	20049	
Independent reflections	3657 [R(int) = 0.0562]	
Completeness to theta = 25.242°	100.0 %	
Absorption correction	Semi-empirical from equivalents	
Max. and min. transmission	0.7456 and 0.6820	
Refinement method	Full-matrix least-squares on F^2	
Data / restraints / parameters	3657 / 0 / 203	
Goodness-of-fit on F^2	1.028	
Final R indices [I>2sigma(I)]	R1 = 0.0481, wR2 = 0.1133	
R indices (all data)	R1 = 0.0760, wR2 = 0.1256	
Extinction coefficient	n/a	
Largest diff. peak and hole	1.015 and -0.470 e.$Å^{-3}$	

Table S2. Crystal data and structure refinement for **4**.

Identification code	d17166_a	
Empirical formula	C52 H78 Cl4 Co2 N4 P2	
Formula weight	1080.78	
Temperature	150(2) K	
Wavelength	0.71073 Å	
Crystal system	Triclinic	
Space group	P-1	
Unit cell dimensions	a = 8.1738(5) Å	a= 103.832(3)°.
	b = 10.2012(5) Å	b= 97.260(3)°.
	c = 17.1703(11) Å	g = 94.369(6)°.
Volume	1370.60(14) $Å^3$	
Z	1	
Density (calculated)	1.309 Mg/m^3	
Absorption coefficient	0.896 mm^{-1}	
F(000)	570	
Crystal size	0.16 x 0.12 x 0.10 mm^3	
Theta range for data collection	2.069 to 27.631°.	
Index ranges	-10<=h<=10, -13<=k<=13, -22<=l<=22	
Reflections collected	33862	
Independent reflections	6311 [R(int) = 0.0447]	
Completeness to theta = 25.242°	99.8 %	
Absorption correction	Semi-empirical from equivalents	
Max. and min. transmission	0.7456 and 0.7047	
Refinement method	Full-matrix least-squares on F^2	
Data / restraints / parameters	6311 / 0 / 294	
Goodness-of-fit on F^2	1.142	
Final R indices [I>2sigma(I)]	R1 = 0.0503, wR2 = 0.1196	
R indices (all data)	R1 = 0.0770, wR2 = 0.1299	
Extinction coefficient	n/a	
Largest diff. peak and hole	0.359 and -0.391 e.$Å^{-3}$	

Table S3. Crystal data and structure refinement for **5**.

Identification code	d17172a_a_tw	
Empirical formula	C30 H54 Cl4 Co2 N4 P2	
Formula weight	792.37	
Temperature	100(2) K	
Wavelength	1.54178 Å	
Crystal system	Triclinic	
Space group	P-1	
Unit cell dimensions	a = 7.8917(3) Å	a= 77.9480(10)°.
	b = 8.7060(3) Å	b= 79.0470(10)°.
	c = 14.1523(5) Å	g = 88.846(2)°.
Volume	933.39(6) $Å^3$	
Z	1	
Density (calculated)	1.410 Mg/m^3	
Absorption coefficient	10.601 mm^{-1}	
F(000)	414	
Crystal size	0.100 x 0.080 x 0.020 mm^3	
Theta range for data collection	3.252 to 66.996°.	
Index ranges	-9<=h<=9, -10<=k<=10, -8<=l<=16	
Reflections collected	3253	
Independent reflections	3253 [R(int) = 0.0795]	
Completeness to theta = 66.996°	97.9 %	
Absorption correction	Semi-empirical from equivalents	
Max. and min. transmission	0.7529 and 0.5068	
Refinement method	Full-matrix least-squares on F^2	
Data / restraints / parameters	3253 / 0 / 195	
Goodness-of-fit on F^2	1.051	
Final R indices [I>2sigma(I)]	R1 = 0.0401, wR2 = 0.0993	
R indices (all data)	R1 = 0.0446, wR2 = 0.1025	
Extinction coefficient	n/a	
Largest diff. peak and hole	0.420 and -0.445 $e.Å^{-3}$	

Table S4. Crystal data and structure refinement for **6**.

Identification code	d1844_a	
Empirical formula	C23 H21 Cl2 Co N2 P	
Formula weight	486.22	
Temperature	150(2) K	
Wavelength	0.71073 Å	
Crystal system	Monoclinic	
Space group	$P2_1/c$	
Unit cell dimensions	a = 10.1359(8) Å	a= 90°.
	b = 11.6672(11) Å	b= 96.513(2)°.
	c = 18.8632(16) Å	g = 90°.
Volume	2216.3(3) $Å^3$	
Z	4	
Density (calculated)	1.457 Mg/m^3	
Absorption coefficient	1.100 mm^{-1}	
F(000)	996	
Crystal size	0.150 x 0.080 x 0.080 mm^3	
Theta range for data collection	2.022 to 27.585°.	
Index ranges	-13<=h<=12, -15<=k<=15, -24<=l<=22	
Reflections collected	27651	
Independent reflections	5103 [R(int) = 0.1032]	
Completeness to theta = 25.242°	100.0 %	
Absorption correction	Semi-empirical from equivalents	
Max. and min. transmission	0.7456 and 0.6489	
Refinement method	Full-matrix least-squares on F^2	
Data / restraints / parameters	5103 / 0 / 265	
Goodness-of-fit on F^2	0.981	
Final R indices [I>2sigma(I)]	R1 = 0.0376, wR2 = 0.0748	
R indices (all data)	R1 = 0.1052, wR2 = 0.0938	
Extinction coefficient	n/a	
Largest diff. peak and hole	0.563 and -0.494 $e.Å^{-3}$	

Table S5. Crystal data and structure refinement for **7**.

Identification code	d1816_a	
Empirical formula	C24 H35 Cl4 Co N2 P	
Formula weight	583.24	
Temperature	150(2) K	
Wavelength	0.71073 Å	
Crystal system	Monoclinic	
Space group	$P2_1/c$	
Unit cell dimensions	a = 18.9295(18) Å	a= 90°.
	b = 11.5800(10) Å	b= 97.447(3)°.
	c = 12.5645(11) Å	g= 90°.
Volume	2731.0(4) $Å^3$	
Z	4	
Density (calculated)	1.419 Mg/m^3	
Absorption coefficient	1.094 mm^{-1}	
F(000)	1212	
Crystal size	0.200 x 0.150 x 0.090 mm^3	
Theta range for data collection	2.066 to 27.592°.	
Index ranges	-24<=h<=24, -15<=k<=15, -16<=l<=14	
Reflections collected	31753	
Independent reflections	6283 [R(int) = 0.0674]	
Completeness to theta = 25.242°	100.0 %	
Absorption correction	Semi-empirical from equivalents	
Max. and min. transmission	0.7456 and 0.6213	
Refinement method	Full-matrix least-squares on F^2	
Data / restraints / parameters	6283 / 380 / 404	
Goodness-of-fit on F^2	1.087	
Final R indices [I>2sigma(I)]	R1 = 0.0668, wR2 = 0.1524	
R indices (all data)	R1 = 0.1229, wR2 = 0.1757	
Extinction coefficient	n/a	
Largest diff. peak and hole	0.847 and -0.769 $e.Å^{-3}$	

Table S6. Crystal data and structure refinement for **8**[a].

Identification code	d1834_b_sq	
Empirical formula	C21.50 H35 Cl2 Co N2 P	
Formula weight	482.31	
Temperature	150(2) K	
Wavelength	1.54178 Å	
Crystal system	Orthorhombic	
Space group	$P2_12_12_1$	
Unit cell dimensions	a = 7.8587(4) Å	□= 90°.
	b = 19.4737(9) Å	□= 90°.
	c = 30.7593(14) Å	□ = 90°.
Volume	4707.3(4) $Å^3$	
Z	8	
Density (calculated)	1.361 Mg/m^3	
Absorption coefficient	8.508 mm^{-1}	
F(000)	2032	
Crystal size	0.320 x 0.050 x 0.020 mm^3	
Theta range for data collection	2.685 to 67.364°.	
Index ranges	-8<=h<=9, -23<=k<=23, -36<=l<=36	
Reflections collected	96373	
Independent reflections	8368 [R(int) = 0.0884]	
Completeness to theta = 67.364°	99.0 %	
Absorption correction	Semi-empirical from equivalents	
Max. and min. transmission	0.7529 and 0.4352	
Refinement method	Full-matrix least-squares on F^2	
Data / restraints / parameters	8368 / 0 / 468	
Goodness-of-fit on F^2	1.051	
Final R indices [I>2sigma(I)]	R1 = 0.0362, wR2 = 0.0798	
R indices (all data)	R1 = 0.0450, wR2 = 0.0851	
Absolute structure parameter	0.490(6)	
Extinction coefficient	n/a	
Largest diff. peak and hole	0.422 and -0.334 $e.Å^{-3}$	

[a] During the refinement of the structure, electron density peaks were located that were believed to be highly disordered solvent molecules. Pentane was the crystallization solvent used. Attempts made to model the solvent molecule were not successful. The SQUEEZE (Spek, 2015) option in PLATON (Spek, 2009) indicated there was a large solvent cavity of 167 A**3. In the final cycles of refinement, this contribution of 51 electrons to the electron density was removed from the observed data. The contribution of one pentane molecule for both independent molecules was added to the empirical formula to adjust the density, the F(000) value and the molecular weight.

Table S7. Crystal data and structure refinement for **9**.

Identification code	d1819_a	
Empirical formula	C17 H25 Cl2 Fe N2 P	
Formula weight	415.11	
Temperature	150(2) K	
Wavelength	1.54178 Å	
Crystal system	Monoclinic	
Space group	$P2_1/n$	
Unit cell dimensions	a = 9.4667(3) Å	a= 90°.
	b = 14.2123(5) Å	b= 103.426(2)°.
	c = 14.8138(6) Å	g = 90°.
Volume	1938.63(12) $Å^3$	
Z	4	
Density (calculated)	1.422 Mg/m^3	
Absorption coefficient	9.543 mm^{-1}	
F(000)	864	
Crystal size	0.100 x 0.030 x 0.030 mm^3	
Theta range for data collection	4.369 to 67.274°.	
Index ranges	-11<=h<=11, -16<=k<=16, -17<=l<=15	
Reflections collected	34968	
Independent reflections	3422 [R(int) = 0.0482]	
Completeness to theta = 67.274°	98.4 %	
Absorption correction	Semi-empirical from equivalents	
Max. and min. transmission	0.7529 and 0.5509	
Refinement method	Full-matrix least-squares on F^2	
Data / restraints / parameters	3422 / 3 / 246	
Goodness-of-fit on F^2	1.020	
Final R indices [I>2sigma(I)]	R1 = 0.0257, wR2 = 0.0612	
R indices (all data)	R1 = 0.0311, wR2 = 0.0642	
Extinction coefficient	n/a	
Largest diff. peak and hole	0.292 and -0.281 e. $Å^{-3}$	

Table S8. Crystal data and structure refinement for **10**.

Identification code	d18123_a	
Empirical formula	C48 H46 Cl8 Fe2 N4 P2	
Formula weight	1136.13	
Temperature	150(2) K	
Wavelength	1.54178 Å	
Crystal system	Monoclinic	
Space group	$P2_1/n$	
Unit cell dimensions	a = 10.4998(3) Å	a= 90°.
	b = 9.7331(3) Å	b= 96.835(2)°.
	c = 24.6015(6) Å	g = 90°.
Volume	2496.30(12) $Å^3$	
Z	2	
Density (calculated)	1.512 Mg/m^3	
Absorption coefficient	9.511 mm^{-1}	
F(000)	1160	
Crystal size	0.070 x 0.070 x 0.030 mm^3	
Theta range for data collection	3.619 to 67.153°.	
Index ranges	-12<=h<=12, -11<=k<=11, -29<=l<=29	
Reflections collected	49628	
Independent reflections	4436 [R(int) = 0.0892]	
Completeness to theta = 67.153°	99.2 %	
Absorption correction	Semi-empirical from equivalents	
Max. and min. transmission	0.7529 and 0.5626	
Refinement method	Full-matrix least-squares on F^2	
Data / restraints / parameters	4436 / 0 / 293	
Goodness-of-fit on F^2	1.051	
Final R indices [I>2sigma(I)]	R1 = 0.0360, wR2 = 0.0897	
R indices (all data)	R1 = 0.0453, wR2 = 0.0938	
Extinction coefficient	n/a	
Largest diff. peak and hole	0.512 and -0.520 e. $Å^{-3}$	

Table S9. Crystal data and structure refinement for **11**.

Identification code	d17169_a	
Empirical formula	C34 H34 Cl2 Fe N2 P2	
Formula weight	659.32	
Temperature	150(2) K	
Wavelength	0.71073 Å	
Crystal system	Triclinic	
Space group	P-1	
Unit cell dimensions	a = 7.5780(8) Å	a= 77.923(4)°.
	b = 12.4245(14) Å	b= 83.039(3)°.
	c = 16.9432(19) Å	g = 81.784(3)°.
Volume	1537.0(3) $Å^3$	
Z	2	
Density (calculated)	1.425 Mg/m^3	
Absorption coefficient	0.796 mm^{-1}	
F(000)	684	
Crystal size	0.190 x 0.060 x 0.060 mm^3	
Theta range for data collection	1.689 to 27.626°.	
Index ranges	-9<=h<=9, -16<=k<=16, -22<=l<=22	
Reflections collected	38943	
Independent reflections	7119 [R(int) = 0.1044]	
Completeness to theta = 25.242°	100.0 %	
Absorption correction	Semi-empirical from equivalents	
Max. and min. transmission	0.7456 and 0.6866	
Refinement method	Full-matrix least-squares on F^2	
Data / restraints / parameters	7119 / 0 / 370	
Goodness-of-fit on F^2	0.998	
Final R indices [I>2sigma(I)]	R1 = 0.0462, wR2 = 0.0709	
R indices (all data)	R1 = 0.1025, wR2 = 0.0850	
Extinction coefficient	n/a	
Largest diff. peak and hole	0.494 and -0.400 e. $Å^{-3}$	

Field-cooled magnetization was measured in an applied field of 1000 Oe over the temperature range of 5-300K using a Quantum Design Magnetic Properties Measurement System (MPMS).

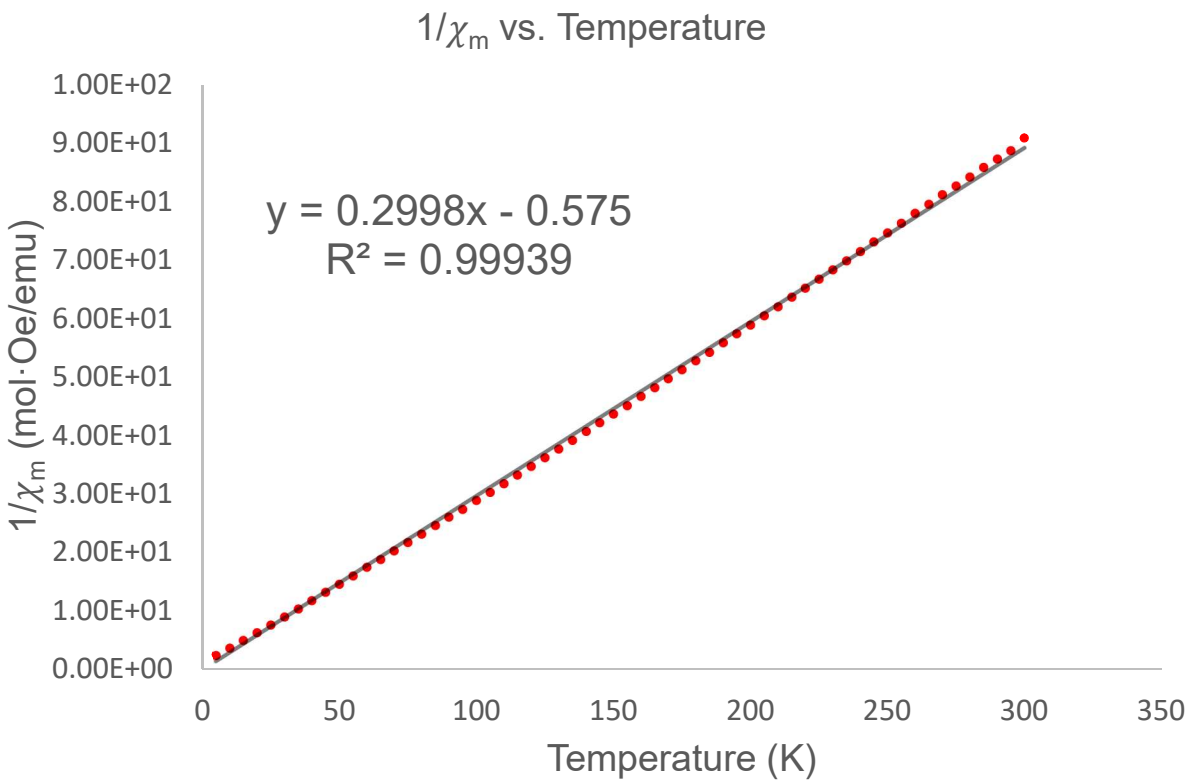

Figure S47. Plot of $1/\chi_m$ vs. T for **9**.

The slope of the curve is equal to 1/C, where C is the Curie constant in Eq 1:

$$\mu_{eff} = \sqrt{\frac{3k_bC}{N\mu_B^2}} \text{ (Eq. 1)}$$

where;
k_b is the Boltzmann constant in CGS units
N is Avogadro's number
μ_B is the Bohr magneton in CGS units

$\mu_{eff} = 5.2\ \mu_B$

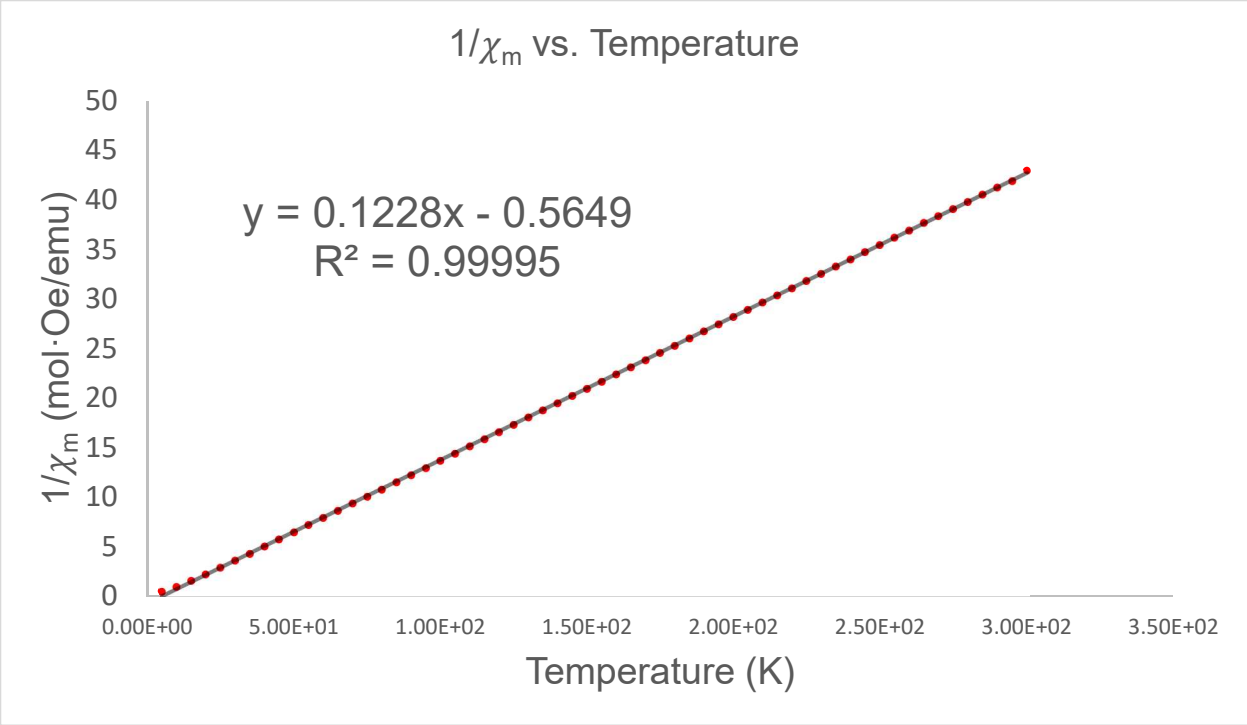

Figure S48. Plot of $1/\chi_m$ vs. T for **10**.

Using Eq. 1

$\mu_{eff} = 7.4\ \mu_B$

Table S10. Magnetic moments of compounds **4-11**. [a] Solution value determined by Evan's Method. [b] Solid state value determined by SQUID.

Compound	**μ_{eff} (μ_B)[a,b]**
Co_2Cl_4(APyPNN-Cy)$_2$ (**4**)	5.4 ± 0.2[a]
Co_2Cl_4(APyPNN-iBu)$_2$ (**5**)	5.8 ± 0.3[a]
$CoCl_2$(AQPNN-Ph) (**6**)	3.9 ± 0.1[a]
$CoCl_2$(AQPNN-Cy) (**7**)	4.2 ± 0.1[a]
$CoCl_2$(AQPNN-iBu) (**8**)	4.2 ± 0.3[a]
$FeCl_2$(AQPNN-iPr) (**9**)	3.9 ± 0.3[a] 5.2[b]
[$FeCl_2$(AQPNN-Ph)]$_2$ (**10**)	7.4[b]
$FeCl_2$(P2NN') (**11**)	4.7 ± 0.3[a]

Base-Study of STAB and Phenyl-Phosphonium Dimer

Visible evolution of hydrogen gas is observed when an equivalent of phenyl-phosphonium dimer (D3) is mixed with 2 equivalents of STAB in THF. The solution bubbles vigorously upon addition of solvent to a mixture of the two solids. ^{11}B NMR shows complete consumption of the starting material at ~-5 ppm (Fig. S49) and generation of two new boron species at -3.1 and 14.5 ppm, the former believed to be $B(OAc)_3$ (Fig. S51). The most closely related compound to $B(OAc)_3$ reported in literature is $B(OPiv)_3$ with a ^{11}B NMR chemical shift of +1.5 ppm.[1]

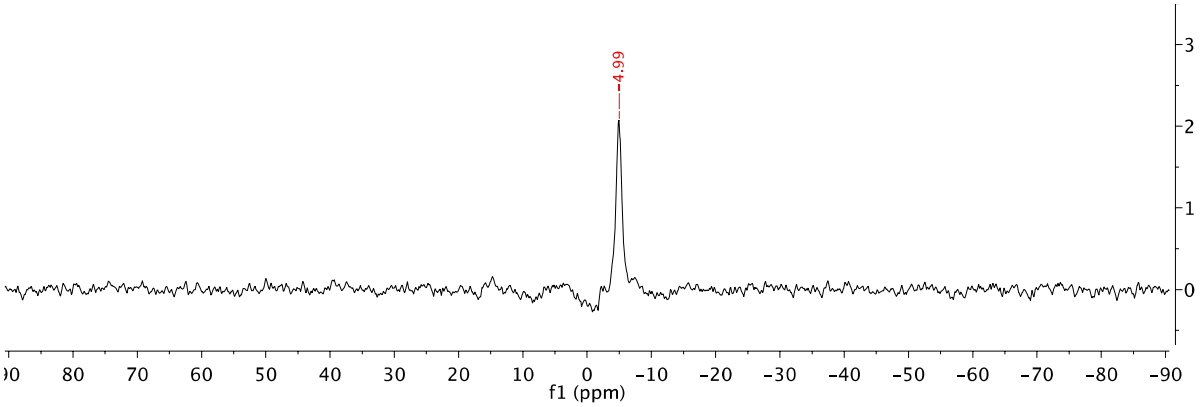

Figure S49. ^{11}B{^{1}H} NMR spectrum (160 MHz, THF) of STAB

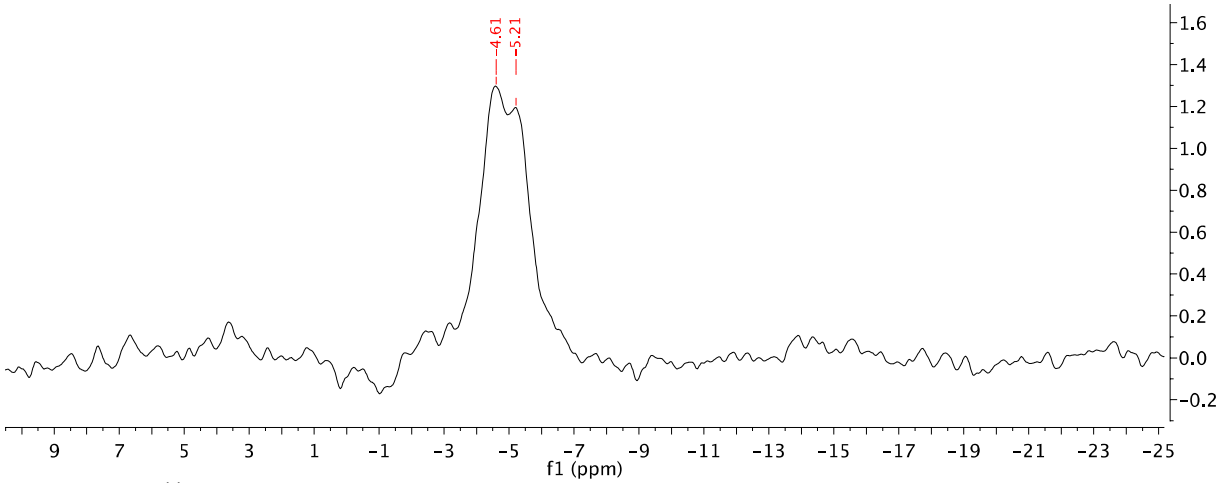

Figure S50. ^{11}B NMR spectrum (160 MHz, THF) of STAB

Fig. S51 is a proton-coupled 11B NMR spectrum and does not show any evidence of splitting due to B-H coupling that is observed in the proton-coupled spectrum of STAB (Fig. S50).

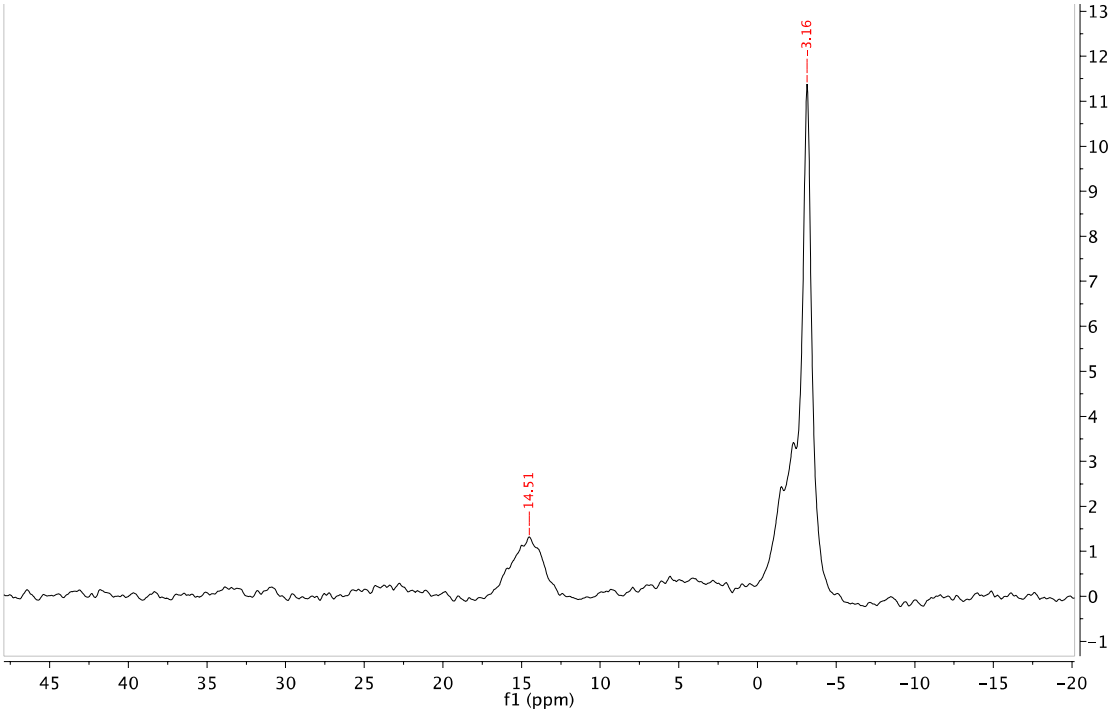

Figure S51. ^{11}B NMR spectrum (160 MHz, THF) of a mixture containing D3 and STAB

Additionally, there is no distinctive observable change in the ^{11}B NMR spectrum of the mixture whether coupling to ^{1}H is turned on or off alluding to the new boron species formed lacking a B–H bond (Fig. S52).

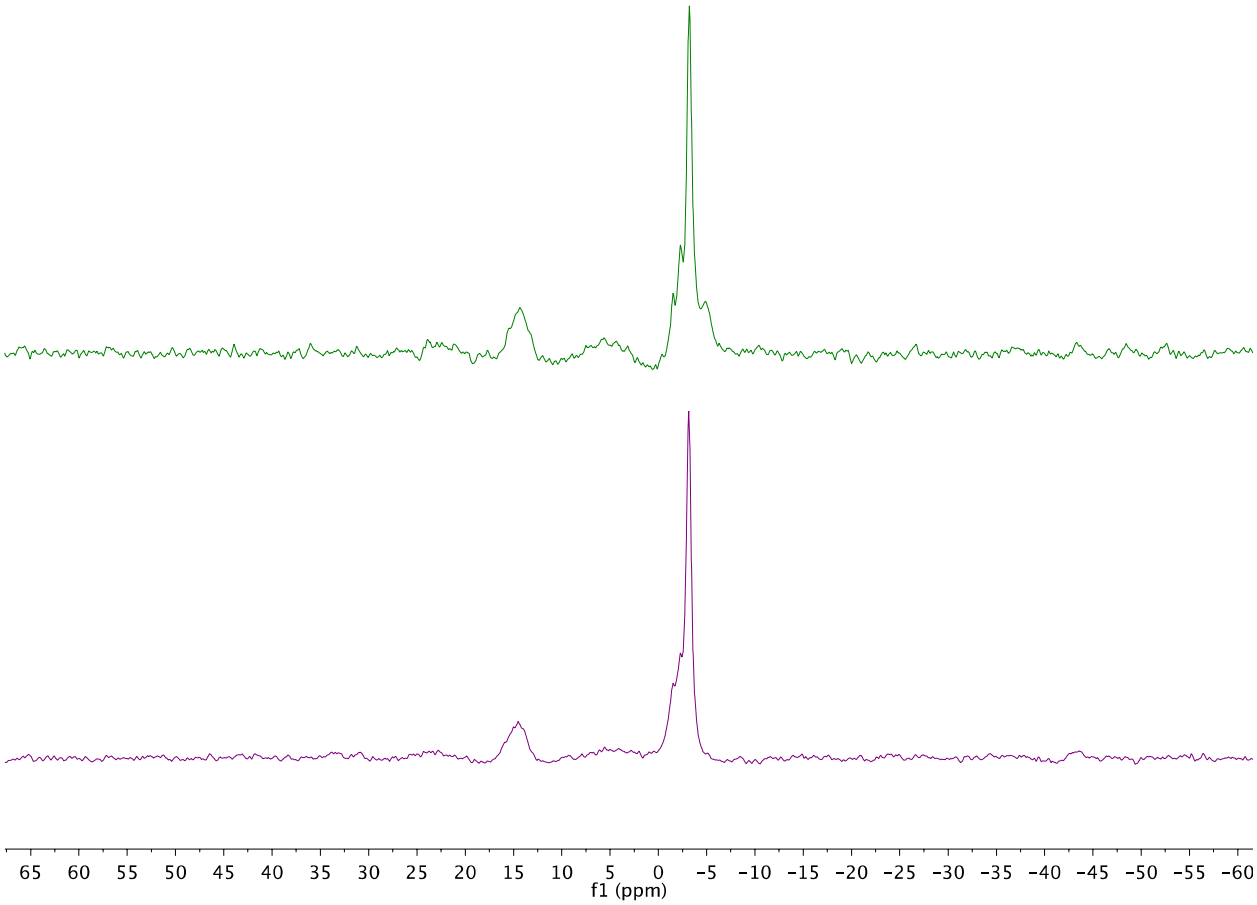

Figure S52. Proton-decoupled (top) and proton-coupled (bottom) ^{11}B NMR spectrum (160 MHz, THF) of mixture containing D3 and STAB.

References:

1. H. C. Brown and T. P. Stocky, *J. Am. Chem. Soc.*, 1977, **99**, 8218–8226.